August 3, 2020

A genome compendium reveals diverse metabolic adaptations of Antarctic soil microorganisms

Maximiliano Ortiz[1 #], Pok Man Leung[2 # *], Guy Shelley[3], Marc W. Van Goethem[1,4], Sean K. Bay[2], Karen Jordaan[1,5], Surendra Vikram[1], Ian D. Hogg[1,7,8], Thulani P. Makhalanyane[1], Steven L. Chown[6], Rhys Grinter[2], Don A. Cowan[1 *], Chris Greening[2,3 *]

[1] Centre for Microbial Ecology and Genomics, Department of Biochemistry, Genetics and Microbiology, University of Pretoria, Hatfield, Pretoria 0002, South Africa

[2] Department of Microbiology, Monash Biomedicine Discovery Institute, Clayton, VIC 3800, Australia

[3] School of Biological Sciences, Monash University, Clayton, VIC 3800, Australia

[4] Environmental Genomics and Systems Biology Division, Lawrence Berkeley National Laboratory, Berkeley, California, USA

[5] Departamento de Genética Molecular y Microbiología, Facultad de Ciencias Biológicas, Pontificia Universidad Católica de Chile, Alameda 340, Santiago

[6] Securing Antarctica's Environmental Future, School of Biological Sciences, Monash University, Clayton, VIC 3800, Australia

[7] School of Science, University of Waikato, Hamilton 3240, New Zealand

[8] Polar Knowledge Canada, Canadian High Arctic Research Station, Cambridge Bay, NU X0B 0C0, Canada

[#] These authors contributed equally to this work.

* Correspondence may be addressed to:

A/Prof Chris Greening (chris.greening@monash.edu)

Prof Don A. Cowan (don.cowan@up.ac.za)

Pok Man Leung (pok.leung@monash.edu)

Abstract

A surprising diversity and abundance of microorganisms resides in the cold desert soils of Antarctica. The metabolic processes that sustain them, however, are poorly understood. In this study, we used metagenomic and biogeochemical approaches to study the microbial communities in 16 physicochemically diverse mountainous and glacial soils from remote sites in South Victoria Land, north of the Mackay Glacier. We assembled 451 metagenome-assembled genomes from 18 bacterial and archaeal phyla, constituting the largest resource of Antarctic soil microbial genomes to date. The most abundant and prevalent microorganisms are metabolically versatile aerobes that use atmospheric hydrogen and carbon monoxide to meet energy, carbon, and, through metabolic water production, hydration needs. Phylogenetic analysis and structural modelling infer that bacteria from nine phyla can scavenge atmospheric hydrogen using a previously unreported enzyme family, the group 1l [NiFe]-hydrogenases. Consistently, gas chromatography measurements confirmed most soils rapidly consume atmospheric hydrogen and carbon monoxide, and provide the first experimental evidence of methane oxidation in non-maritime Antarctica. We also recovered genomes of microorganisms capable of oxidizing other inorganic compounds, including nitrogen, sulfur, and iron compounds, as well as harvesting solar energy via photosystems and novel microbial rhodopsins. Bacterial lineages defined by symbiotic lifestyles, including Patescibacteria, Chlamydiae, and predatory Bdellovibrionota, were also surprisingly abundant. We conclude that the dominant microorganisms in Antarctic soils adopt mixotrophic strategies for energy and sometimes carbon acquisition, though they co-exist with diverse bacteria and archaea that adopt more specialist lifestyles. These unprecedented insights and associated genome compendium will inform efforts to protect biodiversity in this continent.

Introduction

Continental Antarctica is a relatively pristine but oligotrophic wilderness [1]. Terrestrial life on the continent is adapted to extremely low temperatures, low water bioavailability, highly limited organic carbon and nitrogen, salt accumulation and seasonal light/dark periodicity [2–4]. These cumulative pressures exclude most macroscopic fauna and flora, and instead microorganisms constitute most of the continent's biodiversity and biomass [5]. While historical observational surveys indicated that few microorganisms existed in terrestrial Antarctica, subsequent molecular studies have uncovered rich and abundant microbial communities, especially in the continent's ice-free regions [6–10]. Antarctic soil communities are comparable to mesophilic soils at the phylum level, with Actinobacteriota, Acidobacteriota, Chloroflexota and Proteobacteria often predominant [2,8,9,11,12]. These communities are highly specialised at lower taxonomic levels [7,8], however, and have unique functional traits [11,13]. Complementary culture-based studies have also isolated a growing number of taxa from the continent, although from relatively few phyla [14–17]. Most community members are assumed to be extremely slow-growing or adopt dormant states to adapt to the physicochemical conditions of the continent [18]. In turn, the formation of a microbial 'seed bank' may provide a means to maintain biodiversity [19,20].

An enduring question is what metabolic strategies enable soil microorganisms to meet energy and carbon needs on this continent [2]. Even in dormant states, cells still require a net energy input to maintain cellular integrity, repair damaged macromolecules, and generate a basal membrane potential [21,22]. Conventionally it was thought that Cyanobacteria and microalgae are the major primary producers in Antarctic soils and that they produce the organic carbon to sustain organoheterotrophic bacteria [2,11]. However, oxygenic photoautotrophs are typically in low abundance (<1% of total bacterial community) outside lithic niches [11,23] and hence are unlikely to produce sufficient organic carbon to sustain the energy and carbon needs of the dominant community members. More recently, some Antarctic soil bacteria were shown to conserve energy and acquire carbon independently of photoautotrophs [12]. Genome-centric metagenomic studies have revealed that bacteria from several phyla, including Actinobacteriota, consume molecular

hydrogen (H_2) and carbon monoxide (CO) from the atmosphere. By liberating electrons from these ubiquitous and diffusible trace gases, these bacteria sustain aerobic respiration and fix carbon even when preferred organic substrates are limiting [12,24]. However, given the relatively few metagenome-assembled genomes (MAGs) recovered (21) and limited geographical scope of this previous study [12], it is unknown whether trace gas oxidation is a widespread strategy among Antarctic bacteria. Several molecular and biogeochemical studies have detected signatures of carbon fixation through the Calvin-Benson-Bassham (CBB) cycle within the continent, though it is unclear whether this originates through activities of photoautotrophs or lithoautotrophs [12,13,25–27]. Molecular evidence also suggests that some Antarctic soil bacteria can also conserve energy through other means, including methanotrophy, nitrification, and rhodopsin-based light harvesting [12,13,16,28–30].

Here we build on these initial findings to develop a holistic genome-resolved understanding of the metabolic capabilities of Antarctic soil microorganisms. We profiled 16 soils with distinct physicochemical properties from the Mackay Glacier region, a cold hyper-arid ice-free region to the north of the McMurdo Dry Valleys that comprises approximately 15% (~4,800 km^2) of the ice-free regions on the continent. Soil microbial communities in this region are adapted to average annual temperatures of -20°C and annual precipitation below 50 mm [31,32], as well as profound limitation for organic carbon (~0.1%) and nitrogen (~0.02%) [33]. Through deep metagenomic sequencing, we generated a resource of 451 metagenome-assembled genomes, covering all major microbial lineages in the region. We confirmed that the most abundant bacteria in the region are mixotrophs that scavenge atmospheric trace gases, and substantiated these findings with biogeochemical assays confirming rapid gas consumption and phylogenetic analyses revealing a novel hydrogenase family. These findings lend strong support to the recent hypothesis that survival in desert soils depends on continual harvesting of alternative energy sources [18]. Nevertheless, these metabolically versatile bacteria co-exist with microorganisms that adopt a wide range of other nutritional and ecological strategies, including apparent obligate parasites and predators. Altogether, Antarctic soils appear to harbour much more compositionally rich and functionally complex microbial life than previously assumed.

Results and Discussion

Genome-resolved metagenomics reveals phylogenetically diverse bacteria co-exist across the Mackay Glacier region

We analyzed surface soils from sixteen glacial and mountainous sites sampled across the Mackay Glacier region of South Victoria Land. Physicochemical analysis confirmed that the soils varied in key properties (e.g. pH, salinity, micronutrients, texture), but in common with previously characterized soils from continental Antarctic regions[8,34,35], all had exceptionally low organic carbon content (0.02 – 0.25%) (**Table S1**). These soils nevertheless supported moderately abundant bacterial and archaeal communities (1.7×10^6 to 2.7×10^7 16S rRNA gene copies per gram soil wet weight) (**Figure 1a**). Based on high-resolution 16S rRNA amplicon sequencing [36] (**Figure S1a & S1b**), observed richness (832 ± 258) and Shannon index (5.27 ± 0.31) were high in most samples, implying diverse community members co-exist in these soils (**Figure 1c; Figure S1d**). Beta diversity analysis confirmed microbial communities diverge between sampled regions and with geographic distance (**Figure 1d; Figure S1e**).

To determine the community composition of the samples, we retrieved and classified shotgun metagenomic reads of the universal single-copy ribosomal protein gene *rplP* (**Table S2**). The dominant community members were from bacterial phyla known to predominate in soil ecosystems [37,38]. Actinobacteriota, Proteobacteria, Acidobacteriota, Chloroflexota, Gemmatimonadota, Verrucomicrobiota and Bacteroidota were particularly abundant (**Figure 1b**), in agreement with other Antarctic surveys [2,18]. Cyanobacteria were scarce in most soils except for Pegtop Mountain and Cliff Nunatak, accounting for an average of 0.50% in the soil communities. Likewise, Archaea were minor members of this ecosystem (av. 0.88%) and mainly comprised the ammonia-oxidizing order Nitrososphaerales (**Figure 1b**). More surprisingly, bacterial phyla that predominantly adopt a predatory (Bdellovibrionota) [39], intracellular parasitic (Dependentiae and Verrucomicrobiota_A / Chlamydiae) [40,41] or obligately symbiotic (Patescibacteria) [42,43] lifestyle were prevalent and sometimes highly abundant, for example together comprising 17% of the community at Mount Murray. This suggests that a range of symbiotic interactions

occur in these communities. These dominant and rare phyla were also detected by 16S rRNA gene sequencing **(Figure S1c; Table S3**).

These inferences on the composition and metabolic capabilities of the microbial communities were supported by genome-resolved analysis. From the 99.5 gigabases of sequencing data (**Table S4**), we reconstructed a non-redundant set of 101 high-quality and 350 medium-quality [44] metagenome-assembled genomes (MAGs). The recovered genomes span 18 different phyla, the relative composition of which reflects the community structure patterns observed in the *rplP* and 16S rRNA analysis (**Figure 1b**). In turn, they capture all major microbial lineages (present at >1% relative abundance across all samples) and map to an average of 26% of reads in each metagenome (**Table S5**). To the best of our knowledge, this represents the largest sequencing effort and most extensive genomic resource reported from terrestrial Antarctica to date.

Most abundant lineages encode enzymes supporting trace gas oxidation, including a novel family of [NiFe]-hydrogenases

We sought to understand which metabolic strategies support the numerous bacteria in these hyper-oligotrophic soils. We profiled the distribution and affiliation of 52 conserved marker genes representing different energy conservation and carbon acquisition pathways in both the metagenomic short reads (**Table S6**) and MAGs (**Table S5**). In line with expectations, almost all community members encoded genes for aerobic organotrophic respiration (CoxA, NuoF, SdhA, AtpA) (**Figure 2**), whereas capacity for anaerobic respiration and fermentation was low (**Figure S2**). In addition to formate dehydrogenase, the other most abundant markers were the catalytic subunits of [NiFe]-hydrogenases (present in average of 90% community members), form I carbon monoxide dehydrogenases (32%), and RuBisCO (27%) (**Figure 2**). Phylogenetic analysis revealed that most binned sequences of these enzymes were most closely related to clades that support atmospheric H_2 oxidation [45–49] (**Figure 3a**), atmospheric CO oxidation [12,50–53] (**Figure S3**), and chemosynthetic CO_2 fixation [12,54–56] (**Figure S4**). Recent pure culture studies have shown that energy liberated by atmospheric H_2 and CO oxidation supports bacterial persistence during carbon starvation and, in some cases, mixotrophic growth [52,57–62]. Thus, the ability of

bacteria to harvest these trace gases may confer a major selective advantage in the carbon-depleted soils of Antarctica. Moreover, in extension of findings made in the Windmill Islands region [12], over a quarter of the community may fix carbon via the CBB cycle, providing a mean to generate biomass independently of photoautotrophy.

Genes for trace gas oxidation were present in the most abundant and widespread community members. Uptake hydrogenases were encoded by MAGs affiliating with nine bacterial phyla (**Figure 2 & 3a**), including the seven dominant soil phyla (**Figure 1**), whereas CO dehydrogenases were confined to Actinobacteriota and Chloroflexota (**Figure S3**). Indeed, 17 of the 20 most abundant Actinobacteriota and Chloroflexota MAGs encoded one or both enzymes (**Table S5**). Remarkably, the CBB pathway (**Figure S4; Table S7**) frequently co-occurs with hydrogenases (64%) and CO dehydrogenase (25%) in MAGs (**Figure 2; Table S5**), potentially enabling hydrogenotrophic, carboxydotrophic or mixotrophic growth. This association was especially pronounced in the uncultivated classes Ellin6529 (Chloroflexota) and UBA4738 (Actinobacteriota) (**Table S6**), which respectively comprise an average of 5.1% and 0.9% (maximum of 12.3% and 2.4%) of the communities across the region (**Table S2**). These classes are predicted to couple atmospheric H_2 and CO oxidation to fix carbon via their respective type IC and IE RuBisCO enzymes (**Figure S4; Table S7**). These traits in turn may contribute to their unexpectedly high relative abundance in Antarctica as well as other oligotrophic soils [15,63–66]. Indeed, given their abundance in the community and genetic potential for atmospheric chemosynthesis [12,24], we hypothesize that both classes are major Antarctic primary producers. We propose replacing the placeholder names UBA4738 with *Candidatus* Aridivitia (arid Actinobacteriota class; based on high-quality type MAG MGR_bin238, '*Candidatus* Aridivita willemsiae') and Ellin6529 with *Candidatus* Edaphomicrobia (edaphic Chloroflexota class; based on high-quality type MAG MGR_130 '*Candidatus* Edaphomicrobium janssenii') (**Etymological Information**), as per recent taxonomic recommendations [67,68].

Most microorganisms in the Mackay Glacier region encoded a novel hydrogenase family (**Figure 2**). We generated a maximum-likelihood tree of the conserved catalytic subunits of group 1 [NiFe] hydrogenases using amino acid sequences retrieved from 176 MAGs. All hydrogenase sequences form two major and tremendously diverse lineages that share less than 40% sequence identity with each

other and were supported by robust bootstrapping (**Figure 3a**). One branch is associated with characterized group 1h [NiFe] hydrogenases from multiple bacterial isolates [45–47,51,61]. The other forms a novel cluster, herein the group 1l [NiFe]-hydrogenase, which includes the previously unreported hydrogenases of McMurdo Dry Valleys isolate *Hymenobacter roseosalivarius* [69] and several other recently sequenced isolates. Group 1l is the prevailing hydrogenase family within the Mackay Glacier region, with an estimated abundance 2.3 times higher than group 1h (**Table S5**), and is encoded by all nine hydrogenase-bearing phyla and the two candidate classes. As elaborated in **Supplementary Note 1**, structural modelling shows that this enzyme shares common structural features with previously characterized group 1h [NiFe]-hydrogenase [70,71], but contains large sequence insertions and a key substitution in a residue ligating the proximal iron-sulfur cluster. Even more strikingly, the genes encoding this hydrogenase often have an unusual arrangement (**Figure S5; Table S7**), with five open reading frames predicted to encode small transmembrane proteins separating the small and large core structural subunits. On this basis, we predict that this enzyme is a *bona fide* high-affinity membrane-associated hydrogenase that relays electrons derived from atmospheric H_2 through the respiratory chain. The broad distribution and predominance of this hydrogenase suggests it is the primary mediator of H_2 oxidation in these soils. Moreover, given the strong positive correlation between this hydrogenase and RuBisCO based on the MAGs and metagenomic short reads (R^2 = 0.68, p = 0.002) (**Figure S6; Table S9**), it is likely that electrons yielded by this enzyme support carbon fixation either through direct transfer or reverse electron flow.

Trace gas consumption occurs at sufficient rates to meet energy needs and support hydration of Mackay Glacier region bacteria

Our metagenomic analyses suggest that the most abundant soil bacteria across the Mackay Glacier region conserve energy and fix carbon by oxidizing atmospheric H_2 and CO. To test whether soil communities mediate these activities, we set up soil microcosms in which ambient air headspaces were amended with 10 parts per million (ppmv) of these gases and used high-sensitivity gas chromatography to measure their consumption over time. In line with predictions, H_2 was oxidized by

soils from all sixteen sites and all but three soils consumed CO (**Figure 4a**). Of these, all soils except Pegtop Mountain consumed H_2 to below atmospheric concentrations (0.53 ppmv) [72] and ten soils consumed atmospheric CO (0.09 ppmv) [73] during the timecourse of our experiments (**Figure S7**). These sub-atmospheric thresholds confirm that these microbial communities can harvest energy from the atmosphere, a virtually unlimited source of diffusive and energy-rich reduced gases [74,75]. The average rate of atmospheric H_2 oxidation (135 pmol hr^{-1} $g_{soil\ ww}^{-1}$) was much faster than for atmospheric CO oxidation (0.60 pmol hr^{-1} $g_{soil\ ww}^{-1}$) (**Table S8**). This finding, together with the higher abundance of putative H_2 oxidizers in the soil communities (**Figure 2**), suggests that atmospheric H_2 is likely to be the predominant energy source sustaining these communities. As elaborated in **Supplementary Note 2**, considerable variations in bulk and normalized oxidation rates were measured for both gases, which was significantly correlated with several measured physicochemical variables (**Figure S6; Table S9**).

Cell-specific rates were calculated by normalizing bulk rates against soil microbial abundance and the proportion of trace gas oxidizers. Cell-specific atmospheric H_2 oxidation rates were high (av. 1.1×10^{-7} nmol hr^{-1} $cell^{-1}$) and approximately two orders of magnitude higher than those of CO (av. 1.3×10^{-9} nmol hr^{-1} $cell^{-1}$) (**Figure 4b**). In line with our findings in the Windmill Islands region [12], this rate of atmospheric H_2 consumption exceeds the theoretical maintenance requirements of trace gas oxidizers at the temperature tested (10°C) and is sufficient to support some growth [76–78]. It should also be noted that metabolic water is the major end-product of the aerobic respiration of atmospheric H_2 ($2\ H_2 + O_2 \rightarrow 2\ H_2O$). Given the reported cytosolic orientation of high-affinity hydrogenases and terminal oxidases [62], the water produced would be retained in the cytosol, including as a solvent for macromolecules. Thus, trace gas oxidation may be a simple, but hitherto overlooked, mechanism for microorganisms to stay hydrated in the hyper-arid deserts of Antarctica. Based on cell-specific rates of atmospheric H_2 oxidation, a theoretical average of 1.1 million water molecules would be produced per cell each minute. For a cell with an expected 1 μm^3 volume and 70% water content [79,80], such production rates would be sufficient to replace all cellular water over a 15-day period (**Table S8**). We therefore propose that the metabolic water continuously generated by trace

gas oxidation is a quantitatively significant source of hydration in this environment with minimal precipitation [32].

Metabolically constrained phototrophs, lithotrophs, and organotrophs co-exist with versatile mixotrophs in Antarctic soils

While the most abundant taxa in the Mackay Glacier ecotone appear to be versatile mixotrophs, the genome compendium revealed that these ecosystems also harbor diverse bacteria and archaea with specialist strategies for energy and carbon acquisition. Multiple chemolithoautotrophs were present, including those capable of oxidizing the trace amounts of ammonium, sulfur and iron detected in the soils (**Table S1**). Ammonium and nitrite oxidizers comprised an average of 2.9% and 1.0% of the communities, but together comprised 23% and 15% of the community in Mount Seuss 6 and Benson Glacier samples, respectively (**Figure 2; Table S6**). Phylogenetic analysis confirmed that Nitrososphaerales (archaea) and Burkholderiales (bacteria) were the dominant ammonium oxidizers (**Figure S8**), in line with previous reports for McMurdo Dry Valley soils [28], whereas Nitrospirota were the main nitrite oxidizers (**Figure S9**). These nitrifiers also respectively encoded the signature enzymes to fix carbon through the archaeal 4-hydroxybutyrate cycle (**Figure S10**), proteobacterial CBB cycle (**Figure S4**), and nitrospiral reverse tricarboxylic acid cycle (**Figure S11**), suggesting that multiple chemosynthetic primary production strategies sustain biodiversity in these oligotrophic soils. The marker genes for sulfide and thiosulfate oxidation (Sqr, FCC, SoxB) were each encoded by 1 - 4% of community members in most soils (**Figure 2; Table S5**), including multiple Burkholderiales MAGs and several other lineages (**Figure S12, S13, S14**). The genes to oxidize ferrous iron via the *c*-type cytochrome Cyc2 were widespread in Mount Seuss 6 (4.7%) and Cliff Nunatak samples (7.3%), and present in select MAGs from five major phyla (**Figure S15**). Thus, atmospheric and edaphic inorganic compounds alike are major energy sources for Antarctic soil communities, although their relative importance varies across the physicochemically diverse soils from the region.

Our metagenomic analysis suggests that light energy supports few photoautotrophs, but numerous photoheterotrophs, in the region. Reflecting cyanobacterial

distributions across the region (**Figure 1b**), photosystems associated with oxygenic photosynthesis were encoded by few community members except in the Pegtop Mountain and Cliff Nunatak samples (**Figure 2**). Some photosystem II sequences affiliated with proteobacterial anoxygenic phototrophs were also detected (**Figure S16**). In contrast, energy-converting microbial rhodopsins were prevalent and abundant across the region (**Figure 2**). These light-powered proton pumps are well-characterized for their role in energy conservation in marine and freshwater ecosystems [81–85], though have been scarcely studied in desert environments [86]. As outlined by our 'continual energy harvesting hypothesis', sunlight (in common with atmospheric trace gases) is a relatively dependable energy source and hence lineages that harvest it may have a selective advantage in energy-poor desert soils [18]. In line with this theory, putative energy-converting rhodopsins were present in several of the most dominant orders of Actinobacteriota and Chloroflexota in these soils (**Table S5**). They were also present in both cyanobacterial MAGs, thereby providing a means for photoautotrophs to conserve energy when water for oxygenic photosynthesis is limiting (**Figure S17**). Phylogenetic analysis confirmed the binned and unbinned sequences fell into diverse clades (**Figure S17**), including two novel clades that were most closely related (<50% sequence identity) to the biochemically characterized energy-converting rhodopsins of halophilic archaea (bacteriorhodopsins) [87] and *Pantoea* species (pantorhodopsins) [88].

Twenty metagenome-assembled genomes were also recovered for the phyla known to adopt obligately symbiotic lifestyles, namely Patescibacteria, Chlamydiae, Dependentiae, and Bdellovibrionota (**Table S5**). All four phyla appear to be obligate organoheterotrophs that lack alternative pathways for energy conservation or carbon acquisition (**Figure 2**). Based on previous reports, all characterized Bdellovibrionota predate bacterial species [39], whereas Chlamydiae and Dependentiae are likely to be parasites of protist or arthropod species [40,41,89] such as populations of springtails (Collembola) identified within the same sampling area [90]. Signature genes associated with the symbiotic lifestyles of each MAG were detected, for example host-targeted peptidoglycan metalloendopeptidases and self-protection proteins that Bdellovibrionota uses to invade cells of bacterial prey [91,92], as well as ankyrin repeat and WD40 repeat proteins implicated in modulation of eukaryotic hosts by Dependentiae [41,89] (**Table S5**). Also in line with an obligately symbiotic lifestyle,

317 several lineages have ultra-small genomes when adjusted for completeness, namely
318 the eight Patescibacteria MAGs (av. 1.3 Mbp), three Dependentiae MAGs (av. 1.8
319 Mbp), and a Rickettsiaceae MAG (1.3 Mbp) (**Table S5**), and are predicted to be
320 auxotrophic for multiple amino acids. Building on the discovery of unexpected
321 symbionts in Antarctic lakes [93,94], to our knowledge this is the first report that
322 microbial parasitism is a major ecological strategy in terrestrial Antarctica. We also
323 reveal oxic niches for phyla such as Patescibacteria that have, until now, primarily
324 been studied in anoxic ecosystems [42,95,96].

325 Finally, we obtained genomic and biogeochemical evidence that atmospheric
326 methane oxidation occurs on non-maritime Antarctic soils. Based on methane
327 monooxygenase levels in short reads, aerobic methanotrophs are members of the
328 rare biosphere in most of the sampled Antarctic soils, but are present in very high
329 levels in three soils, including Mount Seuss 5 (9.4%) (**Figure 2; Table S5**).
330 Concordantly, two of these soils oxidized methane at high cell-specific rates to sub-
331 atmospheric levels during microcosm incubations (**Figure 4; Figure S7**). Genome-
332 resolved analysis suggested that this activity is primarily mediated by a single
333 bacterial species within the gammaproteobacterial order UBA7966, which encodes a
334 particulate methane monooxygenase clustering with sequences from the
335 atmospheric methane-oxidizing clade USCγ (**Figure S18**). While this bacterium has
336 a restricted distribution, based on read mapping, it is among the most abundant
337 single taxon across the entire region (**Table S5**). Thus, by adopting a relatively
338 specialist lifestyle dependent on assimilating a widely available but catalytically
339 demanding atmospheric substrate, this bacterium fills a distinct ecological niche.
340 Importantly, although methanotroph genomes have previously been reported in
341 Antarctic soils [12,30], this is the first experimental report that such bacteria are
342 biogeochemically active.

Conclusions

Altogether, these results demonstrate a remarkable diversity of both microbial lineages and metabolic strategies in the resource-poor soils of Antarctica. The most abundant and prevalent bacterial lineages in Antarctic soils appear to be free-living mixotrophs capable of meeting carbon, energy, and even hydration needs from atmospheric trace gases, i.e. 'living on air' [97]. Several bacteria and archaea also achieve high abundances in specific soils through more specialist strategies, spanning atmospheric methanotrophy, oxygenic photosynthesis and lithoautotrophic growth on trace edaphic substrates. This environment in turn has selected for a range of as-yet-uncultivated bacterial lineages (e.g. *Ca.* Edaphomicrobia and *Ca.* Aridivitia) and previously unreported gene families (e.g. encoding group 1l [NiFe]-hydrogenases and potential microbial rhodopsins). Also, surprisingly, a significant minority of community members gain resources through parasitism or predation of microorganisms. Through this combination of strategies, both free-living and symbiotic microorganisms can achieve stable niches in a polyextreme environment.

Additionally, the wealth of metagenomic sequencing data and 451 draft genomes generated by this study provides a valuable resource for two major areas of endeavor. First, these datasets support fundamental research and potentially inform decisions to secure Antarctica's environmental future, given forecasts of changing temperature and water availability [98–100]. Thus, in line with one of the six priorities for Antarctic science [101], this resource will provide insights into how life has evolved and adapted on this microbially-dominated continent, and in turn may respond to climate changes. Secondly, these findings also contribute to considerations of what processes may sustain life on other cold, dry planets such as Mars. Antarctica has long been considered a potential analogue for life elsewhere in the solar system [102]. Our work brings that picture into sharper resolution.

Materials and Methods

Soil physicochemical analysis

This study used mineral soils previously sampled from 16 glacier- or mountain-associated sites in the Mackay Glacier region, South Victoria Land, Antarctica during January 2015 as previously described [33,35]. In brief, 50 g of surface soil (depth: 0 - 5 cm) at each location was collected from an approximately 1 m^2 area and stored in sterile 50 ml polypropylene Falcon tubes (Grenier, Bio-One) aseptically. During storage and transportation to University of Pretoria, samples were kept at -80°C. They were later shipped to Monash University's quarantine approved facilities for further experiments. Details of soil samples can be found in **Table S1**. Prior to physicochemical measurements, approximately 35 g of soil of individual sample was aliquoted. Soil aliquots were treated with gamma irradiation at 50 kGy (Steritech Pty Ltd Victoria, Australia) for compliance with Department of Agriculture, Water and the Environment's quarantine good regulations. They were subsequently shipped to the Environmental Analysis Laboratory (EAL), Southern Cross University, Australia for physicochemical analyses in accordance with ISO/IEC 17025 standard procedures. Physicochemical parameters analysed included: basic soil colour and texture; pH and electrical conductivity (1:5 water); moisture content; total carbon, nitrogen, organic carbon, and organic matter; available calcium, magnesium, potassium, ammonium, nitrate, phosphate, sulfur; exchangeable sodium, potassium, calcium, magnesium, hydrogen, and aluminium; cation exchange capacity; Bray I, Bray II, and Cowell phosphorus; and available micronutrients zinc, manganese, iron, copper, boron, and silicon. These data are summarised in **Table S1**.

Shotgun metagenome sequencing, assembly and binning

Community DNA for metagenomic sequencing was extracted from 0.5 g of soil using the FastDNA SPIN Kit for soil (MP Biomedicals) according to the manufacturer's instructions. An extraction blank control was included. Metagenomic shotgun libraries were prepared using the Nextera XT DNA Sample Preparation Kit (Illumina Inc., San Diego, CA, USA) and subject to paired-end sequencing (2 × 150 bp) on an Illumina NextSeq500 platform at the Australian Centre for Ecogenomics (ACE), University of Queensland. Sequencing yielded 356,941,066 read pairs across the sixteen soil metagenomes and 556 read pairs for the negative control (**Table S4**),

indicating a minimal level of contamination from DNA extraction and sequencing processes. Raw metagenomic sequences were subjected to quality filtering using the BBDuk function of the BBTools v38.80 (https://sourceforge.net/projects/bbmap/); contaminating adapters (k-mer size of 23 and hamming distance of 1), PhiX sequences (k-mer size of 31 and hamming distance of 1), and bases from 3' ends with a Phred score below 20 were trimmed. After removing resultant reads with lengths shorter than 50 bp, 93% high-quality read pairs were retained for downstream analysis. Metagenomic reads from each sample were assembled individually with metaSPAdes v3.14.0 [103] and collectively with MEGAHIT v1.2.9 [104] (min k: 27, max k: 127, k step: 10). To generate corresponding coverage profiles for assembled contigs, short reads were mapped back using Bowtie2 v2.3.5 [105] with default parameters. Subsequently, genome binning was performed using CONCOCT v1.1.0 [106], MaxBin2 v2.2.7 [107], and MetaBAT2 v2.15 [108] on contigs with length over 2000 bp. Resulting bins from the same assembly were then dereplicated using DAS_Tool v1.1.2 [109]. RefineM v0.0.25 [110] was used to remove spurious contigs with incongruent genomic and taxonomic properties. Applying a threshold average nucleotide identity of 99%, bins from different assemblies were consolidated to a non-redundant set of metagenome-assembled genomes (MAGs) using dRep v2.5.4 [111]. Completeness and contamination of MAGs were assessed using CheckM v1.1.2 [112]. In total, 101 high quality (completeness > 90% and contamination < 5%) and 350 medium quality (completeness > 50% and contamination < 10%) [44] MAGs from 18 phyla were recovered. Their corresponding taxonomy was assigned by GTDB-TK v1.3.0 [113] with reference to GTDB R05-RS95 [114]. Open reading frames (ORFs) in MAGs were predicted using Prodigal v2.6.3 [115].

Community analysis

Soil microbial community structures were determined by using both metagenomic and 16S rRNA gene amplicon sequencing. Community profiles in sequenced metagenomes were generated by mapping quality-filtered reads to the universal single copy ribosomal marker genes and clustering at 97% identity using SingleM v.0.12.1 (https://github.com/wwood/singlem). To align with the latest GTDB taxonomy at the time of submission (R05-RS95; release 2020/07), we generated a SingleM package for the single-copy ribosomal protein-encoding gene *rplP*. In brief, all *rplP* sequences from Archaea and Bacteria genomes in GTDB R05-RS95

(https://data.ace.uq.edu.au/public/gtdb/data/releases/release95/95.0/) were downloaded. GraftM v0.12.2 [116] was used to generate a phylogenetic package for the sequences which was then used to make a community classification package by SingleM v.0.12.1. For 16S rRNA gene amplicon sequencing, the DNeasy PowerSoil kit (Qiagen) was used to extract DNA from 0.4 g of soil sample as per manufacturer's instructions. The quality and concentration of DNA extracted were determined using a Nanodrop spectrophotometer (ND-1000) and a Qubit Fluorometer. Quantitative PCR (qPCR) using a 96-well plate in a pre-heated LightCycler 480 Instrument II (Roche, Basel, Switzerland) was used to quantify the copy number of the 16S rRNA genes in the samples as previously described [117]. For each sample, the V4 hypervariable region for 16S rRNA gene was amplified using the universal Earth Microbiome Project primer pairs F515 (Parada) [118] and R806 (Apprill) [119]. Amplicons were sent to paired-end sequencing (2 × 300 bp) on an Illumina MiSeq platform at the Australian Centre for Ecogenomics (ACE), University of Queensland. BBDuk function of the BBTools v38.80 was used to trim adapter sequences and filter PhiX contaminants as described above. The sequences were further processed on the QIIME2 platform (release 2019/07) [120] to resolve amplicon sequence variants (ASVs) through the following steps: (i) striping amplicons primers using cutadapt plugin [121]; (ii) merging paired-end reads using q2-vsearch plugin [122]; (iii) quality filtering using a sliding window of four bases with an average Phred score 20; and (iv) de-noising and truncating sequences at 250 base pairs using deblur [123]. A total of 657,975 reads remained in the dataset (min: 13248, max: 102382) (**Table S3**). For taxonomic assignment, ASVs were independently annotated with trained naïve Bayes classifiers of 16S rRNA reference databases Silva release 138 [124] and Greengenes 13.8 [125] (**Table S3**). Multiple sequence alignment of the sequences and subsequent phylogenetic tree building were performed using MAFFT [126] and FastTree [127], respectively, implemented in QIIME2. We then used R packages phyloseq [128], picante [129], vegan [130], betapart [131] and ggplot2 [132] for downstream statistical analysis and visualizations. Alpha diversity including observed richness, Chao1, Shannon index, and Faith's phylogenetic diversity were computed using estimate_richness function in phyloseq and pd function in picante. For beta diversity analysis, all samples were rarefied at the lowest sample sequencing depth, i.e. 13248 sequences per sample and rarefaction plots before and after rarefaction were shown in **Figure S1a-b**. Bray-Curtis dissimilarity was calculated and visualized using a non-metric

multidimensional scaling ordination (NMDS) plot. To examine community turnover in relations to increasing geographic separation, a distance decay relationship of beta diversity (Bray-Curtis dissimilarity) against pairwise geographic distance was computed using the decay.model function fitted with a negative exponential law function in betapart. A *p* value was calculated using the same function with 999 permutations (**Table S3**).

Functional analysis

To estimate the metabolic capability of the soil communities, metagenomes and derived genomes were searched against custom protein databases of representative metabolic marker genes using DIAMOND v.0.9.31 (query cover > 80%) [133]. Searches were carried out using all quality-filtered unassembled reads with lengths over 140 bp and the ORFs of the 451 MAGs. These genes are involved in sulfur cycling (AsrA, FCC, Sqr, DsrA, Sor, SoxB), nitrogen cycling (AmoA, HzsA, NifH, NarG, NapA, NirS, NirK, NrfA, NosZ, NxrA, NorB), iron cycling (Cyc2, MtrB, OmcB), reductive dehalogenation (RdhA), phototrophy (PsaA, PsbA, energy-converting microbial rhodopsin), methane cycling (McrA, MmoA, PmoA), hydrogen cycling (catalytic subunit of [NiFe]-hydrogenases, catalytic domain of [FeFe]-hydrogenases, and Fe-hydrogenases), isoprene oxidation (IsoA), carbon monoxide oxidation (CoxL, CooS), succinate oxidation (SdhA), fumarate reduction (FrdA), and carbon fixation (RbcL, AcsB, AclB, Mcr, HbsT, HbsC) [48,52,134]. Results were filtered based on an identity threshold of 50%, except for group 4 [NiFe]-hydrogenases, [FeFe]-hydrogenases, CoxL, AmoA, and NxrA (all 60%), PsaA (80%), PsbA and IsoA (70%), and HbsT (75%). Subgroup classification of reads was based on the closest match to the sequences in databases. To search for the presence of an additional set of genes involved in oxidative phosphorylation (AtpA), NADH oxidation (NuoF), aerobic respiration (CoxA, CcoN, CyoA, CydA), formate oxidation (FdhA), arsenic cycling (ARO, ArsC), and selenium cycling (YgfK), corresponding in-house databases were generated for this study. All archaeal and bacterial non-redundant proteins were retrieved from NCBI Refseq protein database release 99 [135], which were then screened by hidden Markov models (HMM) [136], with search cutoff scores as described previously [137]. Resulting hits were manually inspected to remove false positives and genes with lengths that deviated more than 20% from the average were discarded. The search of these genes in unassembled reads and ORFs of

MAGs was carried out using the DIAMOND blastp algorithm with a minimum percentage identity of 60% (NuoF), 70% (AtpA, ARO, YgfK) or 50% (all other databases). Read counts for each gene were normalized to reads per kilobase per million (RPKM) by dividing the actual read count by the total number of reads (in millions) and then dividing by the gene length (in kilobases). In order to estimate the gene abundance in the microbial community, high-quality unassembled reads were also screened for the 14 universal single copy ribosomal marker genes used in SingleM v.0.12.1 and PhyloSift [138] by DIAMOND (query cover > 80%, bitscore > 40) and normalized as above. Subsequently, the average gene copy number of a gene in the community was calculated by dividing the read count for the gene (in RPKM) by the mean of the read counts of the 14 universal single copy ribosomal marker genes (in RPKM).

Phylogenetic analysis

Maximum-likelihood phylogenetic trees were constructed to verify the presence and visualise the evolutionary history of key metabolic genes in the metagenome-assembled genomes and assembled unbinned reads. Trees were constructed using the amino acid sequences for subunits of ten enzymes involved in energy acquisition: group 1 [NiFe]-hydrogenase (HhyL, HylL); form I carbon monoxide dehydrogenase (CoxL), particulate methane monooxygenase (PmoA), ammonia monooxygenase (AmoA), nitrite oxidoreductase (NxrA), sulfide-quinone oxidoreductase (Sqr), flavocytochrome *c* sulfide dehydrogenase (FCC), thiosulfohydrolase (SoxB), iron-oxidizing *c*-type cytochrome (Cyc2), photosystem II (PsbA), and energy-converting rhodopsins. Trees were also constructed of the amino acid sequences for subunits of three enzymes involved in carbon fixation: ribulose 1,5-bisphosphate carboxylase/oxygenase (RuBisCO; RbcL), thaumarchaeotal 4-hydroxybutyrate synthase (HbsT), and ATP-citrate lyase (AclB). In all cases, protein sequences retrieved from the MAGs or assembled metagenome sequences by homology-based searches were aligned against a subset of reference sequences from the custom protein databases using ClustalW [139] in MEGA X [140]. Evolutionary relationships were visualized by constructing maximum-likelihood phylogenetic trees; specifically, initial trees for the heuristic search were obtained automatically by applying Neighbour-Join and BioNJ algorithms to a matrix of pairwise distances estimated using a JTT model, and then selecting the topology

with superior log likelihood value. All residues were used and trees were bootstrapped with 50 replicates. To characterise the genetic context of [NiFe] hydrogenases and ribulose-1,5-bisphosphate carboxylase / oxygenase (RuBisCO) from the MAGs, up to 10 genes upstream and downstream of the catalytic subunits were retrieved. These flanking genes were annotated against Pfam protein family database v33.1 [141] using PfamScan v1.6 [142] and NCBI Refseq protein database release 99 [135] using DIAMOND[133] blastp algorithm (default parameters). Alignments with the highest score were retained and are summarised in **Table S7**. The R package gggenes (https://github.com/wilkox/gggenes) was used to construct gene arrangement diagrams.

Hydrogenase sequence analysis and homology modelling

The amino acid sequence for the large (HylL; GBID = SMB94678) and small subunits (HylS GBID = SMB94698) of the group 1l [NiFe]-hydrogenase from *H. roseosalivarius* were inputted into the Phyre2 webserver using default parameters [143]. The highest confidence output model for both subunits was derived from the structure of the group 1h [NiFe]-hydrogenase (HhyLS) from *Cupriavidus necator* H16 (PDB ID = 5AA5) [71]. The structure of the group 1l [NiFe]-hydrogenase tetramer was assembled using Pymol, based on the tetrameric structure of the *C. necator* group 1h [NiFe]-hydrogenase for further analysis. To identify transmembrane helix presence, position and topology in the HylTM proteins associated with group 1l [NiFe]-hydrogenases, the amino acid sequences from *H. roseosalivarius* were inputted into the TMHHM 2.0 webserver [144].

Gas chromatography assays

Soil microcosms were used to determine the capacity of soil microbial communities to oxidize H_2, CO, and CH_4 by gas chromatography. For each of the 16 Mackay Glacier region samples in technical duplicate, 2 g of soil was placed in a 120 ml serum vial and incubated at 10°C. The ambient air headspace was amended with H_2, CO, and CH_4 (via a mixed gas cylinder containing 0.1 % v/v H_2, CO, and CH_4 each in N_2, BOC Australia) to give starting mixing ratios of approximately 10 parts per million (ppmv) for each gas. At each time interval, 2 ml of headspace gas was sampled using a gas-tight syringe and stored in sealed a 3 ml glass exetainer that had been flushed with ultra-high purity N_2 (99.999% pure, BOC Australia) prior to

572 measurement. A VICI gas chromatographic machine with a pulsed discharge helium
573 ionization detector (model TGA-6791-W-4U-2, Valco Instruments Company Inc.) and
574 an autosampler was used to measure gas concentrations as previously described [51].
575 The machine was calibrated against ultra-pure H_2, CO and CH_4 standards down to
576 the limit of quantification (H_2: 20 ppbv; CO: 9 ppbv; CH_4: 500 ppbv). Calibration
577 mixed gas (10.20 ppmv of H_2, 10.10 ppmv of CH_4, 9.95 ppmv of CO in N_2, Air
578 Liquide Australia) and pressurized air (Air Liquide Australia) with known trace gas
579 concentrations were used as internal reference standards. Four pooled heat-killed
580 soils (2 g of pooled soil; treated at 121°C, 15 p.s.i. for 60 mins) were prepared as
581 negative controls. For kinetic analysis, measurement time points with individual gas
582 concentration over 0.4 ppmv were used. First order reaction rate constants were
583 calculated by fitting an exponential model as determined by the lowest overall Akaike
584 information criterion value when compared to a linear model. Actual reaction rate
585 constants of the sample were obtained by correcting against means of negative
586 controls and only resultant values higher than the magnitude of measurement errors
587 of negative controls were retained. Bulk atmospheric gas oxidation rate for each
588 sample was calculated with respect to mean atmospheric mixing ratio of
589 corresponding trace gases (H_2: 0.53 ppmv; CO: 0.09 ppmv; CH_4: 1.9 ppmv) [73,145,146].
590 Soil cell abundance was estimated using 16S rRNA gene copy number from qPCR
591 corrected with a reported average number of 16S rRNA gene copy per genome (i.e.
592 4.2) [147]. Cell specific gas oxidation rates were then inferred by dividing estimated soil
593 cell abundance and the proportion of corresponding gas oxidizers from metagenomic
594 data. To identify factors potentially influencing gas oxidation rates, a two-tailed all-vs-
595 all Spearman correlation matrix was generated that encompassed gas oxidation
596 rates, gas oxidation gene abundances, and soil physicochemical variables for each
597 of the 16 samples.

References

1. Leihy, R. I. *et al.* Antarctica's wilderness fails to capture continent's biodiversity. *Nature* **583**, 567–571 (2020).

2. Cary, S. C., McDonald, I. R., Barrett, J. E. & Cowan, D. A. On the rocks: the microbiology of Antarctic Dry Valley soils. *Nat. Rev. Microbiol.* **8**, 129–138 (2010).

3. Convey, P. *et al.* The spatial structure of Antarctic biodiversity. *Ecol. Monogr.* **84**, 203–244 (2014).

4. Cavicchioli, R. On the concept of a psychrophile. *ISME J.* **10**, 793–795 (2016).

5. Chown, S. L. *et al.* The changing form of Antarctic biodiversity. *Nature* **522**, 431–438 (2015).

6. Cowan, D. A., Russell, N. J., Mamais, A. & Sheppard, D. M. Antarctic Dry Valley mineral soils contain unexpectedly high levels of microbial biomass. *Extremophiles* **6**, 431–436 (2002).

7. Smith, J. J., Tow, L. A., Stafford, W., Cary, C. & Cowan, D. A. Bacterial diversity in three different Antarctic Cold Desert mineral soils. *Microb. Ecol.* **51**, 413–421 (2006).

8. Lee, C. K., Barbier, B. A., Bottos, E. M., McDonald, I. R. & Cary, S. C. The Inter-Valley Soil Comparative Survey: the ecology of Dry Valley edaphic microbial communities. *ISME J.* **6**, 1046–1057 (2012).

9. Ji, M. *et al.* Microbial diversity at Mitchell Peninsula, Eastern Antarctica: a potential biodiversity "hotspot". *Polar Biol.* **33**, 237–249 (2015).

10. Lambrechts, S., Willems, A. & Tahon, G. Uncovering the uncultivated majority in Antarctic soils: toward a synergistic approach. *Front. Microbiol.* **10**, 242 (2019).

11. Pointing, S. B. *et al.* Highly specialized microbial diversity in hyper-arid polar desert. *Proc. Natl. Acad. Sci. U. S. A.* **107**, 1254–1254 (2009).

12. Ji, M. *et al.* Atmospheric trace gases support primary production in Antarctic desert surface soil. *Nature* **552**, 400–403 (2017).

13. Chan, Y., Van Nostrand, J. D., Zhou, J., Pointing, S. B. & Farrell, R. L. Functional ecology of an Antarctic Dry Valley. *Proc. Natl. Acad. Sci. U. S. A.* **110**, 8990–8995 (2013).

14. Peeters, K., Ertz, D. & Willems, A. Culturable bacterial diversity at the Princess Elisabeth station (Utsteinen, Sør Rondane Mountains, East Antarctica) harbours many new taxa. *Syst. Appl. Microbiol.* **34**, 360–367 (2011).

15. Pudasaini, S. *et al.* Microbial diversity of browning Peninsula, Eastern Antarctica revealed using molecular and cultivation methods. *Front. Microbiol.* **8**, 591 (2017).

16. Tahon, G. & Willems, A. Isolation and characterization of aerobic anoxygenic

638 phototrophs from exposed soils from the Sør Rondane Mountains, East
639 Antarctica. *Syst. Appl. Microbiol.* **40**, 357–369 (2017).

640 17. Tahon, G., Tytgat, B., Lebbe, L., Carlier, A. & Willems, A. *Abditibacterium*
641 *utsteinense* sp. nov., the first cultivated member of candidate phylum FBP,
642 isolated from ice-free Antarctic soil samples. *Syst. Appl. Microbiol.* **41**, 279–
643 290 (2018).

644 18. Leung, P. M. *et al.* Energetic basis of microbial growth and persistence in
645 desert ecosystems. *mSystems* **5**, e00495-19 (2020).

646 19. Jones, S. E. & Lennon, J. T. Dormancy contributes to the maintenance of
647 microbial diversity. *Proc. Natl. Acad. Sci. U. S. A.* **107**, 5881–5886 (2010).

648 20. Lennon, J. T. & Jones, S. E. Microbial seed banks: the ecological and
649 evolutionary implications of dormancy. *Nat. Rev. Microbiol.* **9**, 119–130 (2011).

650 21. Rittershaus, E. S. C., Baek, S. H. & Sassetti, C. M. The normalcy of dormancy:
651 common themes in microbial quiescence. *Cell Host and Microbe* vol. 13 643–
652 651 (2013).

653 22. Hoehler, T. M. & Jorgensen, B. B. Microbial life under extreme energy
654 limitation. *Nat. Rev. Microbiol.* **11**, 83–94 (2013).

655 23. Cockell, C. S. & Stokes, M. D. Ecology: Widespread colonization by polar
656 hypoliths. *Nature* **431**, 414 (2004).

657 24. Bay, S., Ferrari, B. & Greening, C. Life without water: How do bacteria
658 generate biomass in desert ecosystems? *Microbiol. Aust.* **39**, (2018).

659 25. Niederberger, T. D. *et al.* Carbon-fixation rates and associated microbial
660 communities residing in arid and ephemerally Wet Antarctic Dry Valley soils.
661 *Front. Microbiol.* **6**, 1347 (2015).

662 26. Tahon, G., Tytgat, B., Stragier, P. & Willems, A. Analysis of *cbbL*, *nifH*, and
663 *pufLM* in Soils from the Sør Rondane Mountains, Antarctica, Reveals a Large
664 Diversity of Autotrophic and Phototrophic Bacteria. *Microb. Ecol.* **71**, 131–149
665 (2016).

666 27. Tahon, G., Tytgat, B. & Willems, A. Diversity of key genes for carbon and
667 nitrogen fixation in soils from the Sør Rondane Mountains, East Antarctica.
668 *Polar Biol.* **41**, 2181–2198 (2018).

669 28. Magalhães, C., Machado, A., Frank-Fahle, B., Lee, C. K. & Cary, C. S. The
670 ecological dichotomy of ammonia-oxidizing archaea and bacteria in the hyper-
671 arid soils of the Antarctic Dry Valleys. *Front. Microbiol.* **5**, 515 (2014).

672 29. Tahon, G., Tytgat, B. & Willems, A. Diversity of phototrophic genes suggests
673 multiple bacteria may be able to exploit sunlight in exposed soils from the Sør
674 Rondane Mountains, East Antarctica. *Front. Microbiol.* **7**, 2026 (2016).

675 30. Edwards, C. R. *et al.* Draft genome sequence of uncultured upland soil cluster
676 *Gammaproteobacteria* gives molecular insights into high-affinity
677 methanotrophy. *Genome Announc.* **5**, e00047-17 (2017).

678 31. Doran, P. T. *et al.* Antarctic climate cooling and terrestrial ecosystem

679 response. *Nature* **415**, 517–520 (2002).

680 32. Fountain, A. G., Nylen, T. H., Monaghan, A., Basagic, H. J. & Bromwich, D.
681 Snow in the McMurdo dry valleys, Antarctica. *Int. J. Climatol. A J. R. Meteorol.*
682 *Soc.* **30**, 633–642 (2010).

683 33. Van Goethem, M. W. *et al.* A reservoir of 'historical' antibiotic resistance genes
684 in remote pristine Antarctic soils. *Microbiome* **6**, 40 (2018).

685 34. Elberling, B. *et al.* Distribution and dynamics of soil organic matter in an
686 Antarctic dry valley. *Soil Biol. Biochem.* **38**, 3095–3106 (2006).

687 35. Adriaenssens, E. M. *et al.* Environmental drivers of viral community
688 composition in Antarctic soils identified by viromics. *Microbiome* **5**, 83 (2017).

689 36. Bay, S. K. *et al.* Soil bacterial communities exhibit strong biogeographic
690 patterns at fine taxonomic resolution. *mSystems* **5**, e00540-20 (2020).

691 37. Janssen, P. H. Identifying the dominant soil bacterial taxa in libraries of 16S
692 rRNA and 16S rRNA genes. *Appl. Environ. Microbiol.* **72**, 1719–1728 (2006).

693 38. Delgado-Baquerizo, M. *et al.* A global atlas of the dominant bacteria found in
694 soil. *Science* **359**, 320–325 (2018).

695 39. Rotem, O., Pasternak, Z. & Jurkevitch, E. The genus Bdellovibrio and like
696 organisms. in *The Prokaryotes: Deltaproteobacteria and Epsilonproteobacteria*
697 vol. 9783642390 3–17 (2014).

698 40. Collingro, A., Köstlbacher, S. & Horn, M. Chlamydiae in the Environment.
699 *Trends Microbiol.* 10.1016/j.tim.2020.05.020 (2020)
700 doi:10.1016/j.tim.2020.05.020.

701 41. Yeoh, Y. K., Sekiguchi, Y., Parks, D. H. & Hugenholtz, P. Comparative
702 genomics of candidate phylum TM6 suggests that parasitism is widespread
703 and ancestral in this lineage. *Mol. Biol. Evol.* **33**, 915–927 (2016).

704 42. Brown, C. T. *et al.* Unusual biology across a group comprising more than 15%
705 of domain *Bacteria*. *Nature* **523**, 208–211 (2015).

706 43. Castelle, C. J. & Banfield, J. F. Major new microbial groups expand diversity
707 and alter our understanding of the tree of life. *Cell* **172**, 1181–1197 (2018).

708 44. Bowers, R. M. *et al.* Minimum information about a single amplified genome
709 (MISAG) and a metagenome-assembled genome (MIMAG) of bacteria and
710 archaea. *Nat. Biotechnol.* **35**, 725–731 (2017).

711 45. Constant, P., Chowdhury, S. P., Pratscher, J. & Conrad, R. Streptomycetes
712 contributing to atmospheric molecular hydrogen soil uptake are widespread
713 and encode a putative high-affinity [NiFe]-hydrogenase. *Environ. Microbiol.* **12**,
714 821–829 (2010).

715 46. Greening, C., Berney, M., Hards, K., Cook, G. M. & Conrad, R. A soil
716 actinobacterium scavenges atmospheric H_2 using two membrane-associated,
717 oxygen-dependent [NiFe] hydrogenases. *Proc. Natl. Acad. Sci. U. S. A.* **111**,
718 4257–4261 (2014).

719 47. Greening, C. *et al.* Persistence of the dominant soil phylum Acidobacteria by

trace gas scavenging. *Proc. Natl. Acad. Sci. U. S. A.* **112**, 10497–10502 (2015).

48. Søndergaard, D., Pedersen, C. N. S. & Greening, C. HydDB: a web tool for hydrogenase classification and analysis. *Sci. Rep.* **6**, 34212 (2016).

49. Constant, P., Chowdhury, S. P., Hesse, L., Pratscher, J. & Conrad, R. Genome data mining and soil survey for the novel Group 5 [NiFe]-hydrogenase to explore the diversity and ecological importance of presumptive high-affinity H_2-oxidizing bacteria. *Appl. Environ. Microbiol.* **77**, 6027–6035 (2011).

50. King, G. M. Molecular and culture-based analyses of aerobic carbon monoxide oxidizer diversity. *Appl. Environ. Microbiol.* **69**, 7257–7265 (2003).

51. Islam, Z. F. *et al.* Two Chloroflexi classes independently evolved the ability to persist on atmospheric hydrogen and carbon monoxide. *ISME J.* **13**, 1801–1813 (2019).

52. Cordero, P. R. F. *et al.* Atmospheric carbon monoxide oxidation is a widespread mechanism supporting microbial survival. *ISME J.* **13**, 2868–2881 (2019).

53. King, G. M. & Weber, C. F. Distribution, diversity and ecology of aerobic CO-oxidizing bacteria. *Nat. Rev. Microbiol.* **5**, 107–118 (2007).

54. Tabita, F. R. *et al.* Function, structure, and evolution of the RubisCO-like proteins and their RubisCO homologs. *Microbiol. Mol. Biol. Rev.* **71**, 576–599 (2007).

55. Park, S. W. *et al.* Presence of duplicate genes encoding a phylogenetically new subgroup of form I ribulose 1,5-bisphosphate carboxylase/oxygenase in *Mycobacterium* sp. strain JC1 DSM 3803. *Res. Microbiol.* **160**, 159–165 (2009).

56. Grostern, A. & Alvarez-Cohen, L. RubisCO-based CO_2 fixation and C1 metabolism in the actinobacterium *Pseudonocardia dioxanivorans* CB1190. *Environ. Microbiol.* **15**, 3040–3053 (2013).

57. Greening, C., Villas-Bôas, S. G., Robson, J. R., Berney, M. & Cook, G. M. The growth and survival of *Mycobacterium smegmatis* is enhanced by co-metabolism of atmospheric H_2. *PLoS One* **9**, e103034 (2014).

58. Liot, Q. & Constant, P. Breathing air to save energy – new insights into the ecophysiological role of high-affinity [NiFe]-hydrogenase in Streptomyces avermitilis. *Microbiologyopen* **5**, 47–59 (2016).

59. Tveit, A. T. *et al.* Widespread soil bacterium that oxidizes atmospheric methane. *Proc. Natl. Acad. Sci. U. S. A.* **116**, 8515–8524 (2019).

60. Islam, Z. F. *et al.* A widely distributed hydrogenase oxidises atmospheric H2 during bacterial growth. *ISME J.* 10.1038/s41396-020-0713–4 (2020) doi:10.1101/2020.04.14.040717.

61. Schmitz, R. A. *et al.* The thermoacidophilic methanotroph *Methylacidiphilum fumariolicum* SolV oxidizes subatmospheric H_2 with a high-affinity, membrane-

associated [NiFe] hydrogenase. *ISME J.* **14**, 1223–1232 (2020).

62. Cordero, P. R. F. *et al.* Two uptake hydrogenases differentially interact with the aerobic respiratory chain during mycobacterial growth and persistence. *J. Biol. Chem.* **294**, 18980–18991 (2019).

63. Lopes, A. R., Manaia, C. M. & Nunes, O. C. Bacterial community variations in an alfalfa-rice rotation system revealed by 16S rRNA gene 454-pyrosequencing. *FEMS Microbiol. Ecol.* **87**, 650–663 (2014).

64. Frindte, K., Pape, R., Werner, K., Löffler, J. & Knief, C. Temperature and soil moisture control microbial community composition in an arctic–alpine ecosystem along elevational and micro-topographic gradients. *ISME J.* **13**, 2031–2043 (2019).

65. Khilyas, I. V. *et al.* Microbial diversity and mineral composition of weathered serpentine rock of the Khalilovsky massif. *PLoS One* **14**, e0225929 (2019).

66. Johnston, E. R. *et al.* Responses of tundra soil microbial communities to half a decade of experimental warming at two critical depths. *Proc. Natl. Acad. Sci.* **116**, 15096–15105 (2019).

67. Whitman, W. B. Modest proposals to expand the type material for naming of prokaryotes. *Int. J. Syst. Evol. Microbiol.* **66**, 2108–2112 (2016).

68. Murray, A. E. *et al.* Roadmap for naming uncultivated Archaea and Bacteria. *Nat. Microbiol.* **5**, 987–994 (2020).

69. Hirsch, P. *et al. Hymenobacter roseosalivarius* gen. nov., sp. nov. from continental Antarctic soils and sandstone: bacteria of the *Cytophaga*/*Flavobacterium*/*Bacteroides* line of phylogenetic descent. *Syst. Appl. Microbiol.* **21**, 374–383 (1998).

70. Schäfer, C., Friedrich, B. & Lenz, O. Novel, oxygen-insensitive group 5 [NiFe]-hydrogenase in Ralstonia eutropha. *Appl. Environ. Microbiol.* **79**, 5137–45 (2013).

71. Schäfer, C. *et al.* Structure of an actinobacterial-type [NiFe]-hydrogenase reveals insight into O_2-tolerant H_2 oxidation. *Structure* **24**, 285–292 (2016).

72. Ehhalt, D. H. & Rohrer, F. The tropospheric cycle of H_2: a critical review. *Tellus B* **61**, 500–535 (2009).

73. Novelli, P. C., Masarie, K. A. & Lang, P. M. Distributions and recent changes of carbon monoxide in the lower troposphere. *J. Geophys. Res. Atmos.* **103**, 19015–19033 (1998).

74. Conrad, R. Soil microorganisms as controllers of atmospheric trace gases (H_2, CO, CH_4, OCS, N_2O, and NO). *Microbiol. Mol. Biol. Rev.* **60**, 609–640 (1996).

75. Greening, C., Grinter, R. & Chiri, E. Uncovering the metabolic strategies of the dormant microbial majority: towards integrative approaches. *mSystems* **4**, e00107-19 (2019).

76. Tijhuis, L., Van Loosdrecht, M. C. & Heijnen, J. J. A thermodynamically based correlation for maintenance gibbs energy requirements in aerobic and

anaerobic chemotrophic growth. *Biotechnol. Bioeng.* **42**, 509–519 (1993).

77. Price, P. B. & Sowers, T. Temperature dependence of metabolic rates for microbial growth, maintenance, and survival. *Proc. Natl. Acad. Sci. U. S. A.* **101**, 4631–4636 (2004).

78. LaRowe, D. E. & Amend, J. P. Power limits for microbial life. *Front. Microbiol.* **6**, 718 (2015).

79. Sundararaj, S. *et al.* The CyberCell Database (CCDB): A comprehensive, self-updating, relational database to coordinate and facilitate in silico modeling of Escherichia coli. *Nucleic Acids Res.* **32**, D293–D295 (2004).

80. Koch, A. L. What size should a bacterium be? A question of scale. *Annu. Rev. Microbiol.* **50**, 317–348 (1996).

81. Finkel, O. M., Béja, O. & Belkin, S. Global abundance of microbial rhodopsins. *ISME J.* **7**, 448–451 (2013).

82. Pinhassi, J., DeLong, E. F., Béjà, O., González, J. M. & Pedrós-Alió, C. Marine bacterial and archaeal ion-pumping rhodopsins: genetic Diversity, physiology, and ecology. *Microbiol. Mol. Biol. Rev.* **80**, 929–954 (2016).

83. Gomez-Consarnau, L. *et al.* Proteorhodopsin Phototrophy Promotes Survival of Marine Bacteria during Starvation. *Plos Biol.* **8**, (2010).

84. Steindler, L., Schwalbach, M. S., Smith, D. P., Chan, F. & Giovannoni, S. J. Energy starved candidatus *Pelagibacter ubique* substitutes light-mediated ATP production for endogenous carbon respiration. *PLoS One* **6**, e19725 (2011).

85. Panwar, P. *et al.* Influence of the polar light cycle on seasonal dynamics of an Antarctic lake microbial community. *Microbiome* 10.1186/s40168-020-00889–8 (2020).

86. Guerrero, L. D., Vikram, S., Makhalanyane, T. P. & Cowan, D. A. Evidence of microbial rhodopsins in Antarctic Dry Valley edaphic systems. *Environ. Microbiol.* **19**, 3755–3767 (2017).

87. Oesterhelt, D. & Stoeckenius, W. Rhodopsin-like protein from the purple membrane of *Halobacterium halobium*. *Nat. new Biol.* **233**, 149–152 (1971).

88. Harris, A. *et al.* A new group of eubacterial light-driven retinal-binding proton pumps with an unusual cytoplasmic proton donor. *Biochim. Biophys. Acta (BBA)-Bioenergetics* **1847**, 1518–1529 (2015).

89. Deeg, C. M. *et al. Chromulinavorax destructans*, a pathogen of microzooplankton that provides a window into the enigmatic candidate phylum Dependentiae. *PLoS Pathog.* **15**, e1007801 (2019).

90. Beet, C. R. *et al.* Genetic diversity among populations of Antarctic springtails (Collembola) within the Mackay Glacier ecotone. *Genome* **59**, 762–770 (2016).

91. Lambert, C. *et al.* Ankyrin-mediated self-protection during cell invasion by the bacterial predator *Bdellovibrio bacteriovorus*. *Nat. Commun.* **6**, 1–10 (2015).

92. Pasternak, Z. *et al.* By their genes ye shall know them: genomic signatures of predatory bacteria. *ISME J.* **7**, 756–769 (2013).

93. Hamm, J. N. *et al.* Unexpected host dependency of Antarctic Nanohaloarchaeota. *Proc. Natl. Acad. Sci.* **116**, 14661–14670 (2019).

94. Lagkouvardos, I. *et al.* Integrating metagenomic and amplicon databases to resolve the phylogenetic and ecological diversity of the Chlamydiae. *ISME J.* **8**, 115–125 (2014).

95. Jaffe, A. L., Castelle, C. J., Carnevali, P. B. M., Gribaldo, S. & Banfield, J. F. The rise of diversity in metabolic platforms across the Candidate Phyla Radiation. *BMC Biol.* **18**, 1–15 (2020).

96. Beam, J. P. *et al.* Ancestral absence of electron transport chains in Patescibacteria and DPANN. *bioRxiv* 2020.04.07.029462 (2020) doi:10.1101/2020.04.07.029462.

97. Cowan, D. A. & Makhalanyane, T. P. Energy from thin air. *Nature* **552**, 336–337 (2017).

98. Lee, J. R. *et al.* Climate change drives expansion of Antarctic ice-free habitat. *Nature* **547**, 49 (2017).

99. Rintoul, S. R. *et al.* Choosing the future of Antarctica. *Nature* **558**, 233–241 (2018).

100. Cavicchioli, R. *et al.* Scientists' warning to humanity: microorganisms and climate change. *Nat. Rev. Microbiol.* **17**, 569–586 (2019).

101. Kennicutt, M. C. 2nd *et al.* Six priorities for Antarctic science. *Nature* **512**, 23–25 (2014).

102. Heldmann, J. L. *et al.* The high elevation Dry Valleys in Antarctica as analog sites for subsurface ice on Mars. *Planet. Space Sci.* **85**, 53–58 (2013).

103. Nurk, S., Meleshko, D., Korobeynikov, A. & Pevzner, P. A. metaSPAdes: a new versatile metagenomic assembler. *Genome Res.* **27**, 824–834 (2017).

104. Li, D. H. *et al.* MEGAHIT v1.0: A fast and scalable metagenome assembler driven by advanced methodologies and community practices. *Methods* **102**, 3–11 (2016).

105. Langmead, B. & Salzberg, S. L. Fast gapped-read alignment with Bowtie 2. *Nat. Methods* **9**, 357 (2012).

106. Alneberg, J. *et al.* Binning metagenomic contigs by coverage and composition. *Nat. Methods* **11**, 1144 (2014).

107. Wu, Y.-W., Simmons, B. A. & Singer, S. W. MaxBin 2.0: an automated binning algorithm to recover genomes from multiple metagenomic datasets. *Bioinformatics* **32**, 605–607 (2015).

108. Kang, D. *et al.* MetaBAT 2: an adaptive binning algorithm for robust and efficient genome reconstruction from metagenome assemblies. *PeerJ* **7**, e7359 (2019).

109. Sieber, C. M. K. *et al.* Recovery of genomes from metagenomes via a dereplication, aggregation and scoring strategy. *Nat. Microbiol.* 1 (2018).

884 110. Parks, D. H. *et al.* Recovery of nearly 8,000 metagenome-assembled genomes
885 substantially expands the tree of life. *Nat. Microbiol.* **2**, 1533 (2017).

886 111. Olm, M. R., Brown, C. T., Brooks, B. & Banfield, J. F. dRep: a tool for fast and
887 accurate genomic comparisons that enables improved genome recovery from
888 metagenomes through de-replication. *ISME J.* **11**, 2864 (2017).

889 112. Parks, D. H., Imelfort, M., Skennerton, C. T., Hugenholtz, P. & Tyson, G. W.
890 CheckM: assessing the quality of microbial genomes recovered from isolates,
891 single cells, and metagenomes. *Genome Res.* **25**, 1043–1055 (2015).

892 113. Chaumeil, P.-A., Mussig, A. J., Hugenholtz, P. & Parks, D. H. GTDB-Tk: a
893 toolkit to classify genomes with the Genome Taxonomy Database.
894 *Bioinformatics* **36**, 1925–1927 (2020).

895 114. Parks, D. H. *et al.* A standardized bacterial taxonomy based on genome
896 phylogeny substantially revises the tree of life. *Nat. Biotechnol.* **36**, 996–1004
897 (2018).

898 115. Hyatt, D. *et al.* Prodigal: prokaryotic gene recognition and translation initiation
899 site identification. *BMC Bioinformatics* **11**, 119 (2010).

900 116. Boyd, J. A., Woodcroft, B. J. & Tyson, G. W. GraftM: a tool for scalable,
901 phylogenetically informed classification of genes within metagenomes. *Nucleic*
902 *Acids Res.* **46**, e59–e59 (2018).

903 117. Chen, Y.-J. *et al.* Metabolic flexibility allows generalist bacteria to become
904 dominant in a frequently disturbed ecosystem. *bioRxiv* 2020.02.12.945220
905 (2020).

906 118. Parada, A. E., Needham, D. M. & Fuhrman, J. A. Every base matters:
907 assessing small subunit rRNA primers for marine microbiomes with mock
908 communities, time series and global field samples. *Environ. Microbiol.* **18**,
909 1403–1414 (2016).

910 119. Apprill, A., McNally, S., Parsons, R. & Weber, L. Minor revision to V4 region
911 SSU rRNA 806R gene primer greatly increases detection of SAR11
912 bacterioplankton. *Aquat. Microb. Ecol.* **75**, 129–137 (2015).

913 120. Bolyen, E. *et al.* Reproducible, interactive, scalable and extensible microbiome
914 data science using QIIME 2. *Nat. Biotechnol.* **37**, 852–857 (2019).

915 121. Martin, M. Cutadapt removes adapter sequences from high-throughput
916 sequencing reads. *EMBnet.journal* **17**, 10 (2011).

917 122. Rognes, T., Flouri, T., Nichols, B., Quince, C. & Mahé, F. VSEARCH: a
918 versatile open source tool for metagenomics. *PeerJ* **4**, 2584 (2016).

919 123. Amir, A. *et al.* Deblur rapidly resolves single-nucleotide community sequence
920 patterns. *mSystems* **2**, e00191-16 (2017).

921 124. Quast, C. *et al.* The SILVA ribosomal RNA gene database project: improved
922 data processing and web-based tools. *Nucleic Acids Res.* **41**, D590–D596
923 (2012).

924 125. McDonald, D. *et al.* An improved Greengenes taxonomy with explicit ranks for

ecological and evolutionary analyses of bacteria and archaea. *ISME J.* **6**, 610–618 (2012).

126. Katoh, K., Misawa, K., Kuma, K. I. & Miyata, T. MAFFT: A novel method for rapid multiple sequence alignment based on fast Fourier transform. *Nucleic Acids Res.* **30**, 3059–3066 (2002).

127. Price, M. N., Dehal, P. S. & Arkin, A. P. FastTree 2 - Approximately maximum-likelihood trees for large alignments. *PLoS One* **5**, (2010).

128. McMurdie, P. J. & Holmes, S. phyloseq: an R package for reproducible interactive analysis and graphics of microbiome census data. *PLoS One* **8**, e61217 (2013).

129. Kembel, S. W. *et al.* Picante: R tools for integrating phylogenies and ecology. *Bioinformatics* **26**, 1463–1464 (2010).

130. Dixon, P. VEGAN, a package of R functions for community ecology. *J. Veg. Sci.* **14**, 927–930 (2003).

131. Baselga, A. & Orme, C. D. L. Betapart: An R package for the study of beta diversity. *Methods Ecol. Evol.* **3**, 808–812 (2012).

132. Wickham, H. *ggplot2: elegant graphics for data analysis*. (Springer, 2016).

133. Buchfink, B., Xie, C. & Huson, D. H. Fast and sensitive protein alignment using DIAMOND. *Nat. Methods* **12**, 59 (2014).

134. Greening, C. *et al.* Diverse hydrogen production and consumption pathways influence methane production in ruminants. *ISME J.* **13**, 2617–2632 (2019).

135. Pruitt, K. D., Tatusova, T. & Maglott, D. R. NCBI reference sequences (RefSeq): a curated non-redundant sequence database of genomes, transcripts and proteins. *Nucleic Acids Res.* **35**, D61–D65 (2007).

136. Eddy, S. R. Accelerated profile HMM searches. *PLoS Comput. Biol.* **7**, e1002195 (2011).

137. Anantharaman, K. *et al.* Thousands of microbial genomes shed light on interconnected biogeochemical processes in an aquifer system. *Nat. Commun.* **7**, 13219 (2016).

138. Darling, A. E. *et al.* PhyloSift: phylogenetic analysis of genomes and metagenomes. *PeerJ* **2**, e243 (2014).

139. Larkin, M. A. *et al.* Clustal W and Clustal X version 2.0. *Bioinformatics* **23**, 2947–2948 (2007).

140. Kumar, S., Stecher, G., Li, M., Knyaz, C. & Tamura, K. MEGA X: molecular evolutionary genetics analysis across computing platforms. *Mol. Biol. Evol.* **35**, 1547–1549 (2018).

141. Finn, R. D. *et al.* Pfam: The protein families database. *Nucleic Acids Research* vol. 42 D222–D230 (2014).

142. Madeira, F. *et al.* The EMBL-EBI search and sequence analysis tools APIs in 2019. *Nucleic Acids Res.* **47**, W636–W641 (2019).

143. Kelley, L. A., Mezulis, S., Yates, C. M., Wass, M. N. & Sternberg, M. J. E. The Phyre2 web portal for protein modeling, prediction and analysis. *Nat. Protoc.* **10**, 845–858 (2015).

144. Krogh, A., Larsson, B., Von Heijne, G. & Sonnhammer, E. L. L. Predicting transmembrane protein topology with a hidden Markov model: Application to complete genomes. *J. Mol. Biol.* **305**, 567–580 (2001).

145. Novelli, P. C. *et al.* Molecular hydrogen in the troposphere: global distribution and budget. *J. Geophys. Res. Atmos.* **104**, 30427–30444 (1999).

146. Stocker, T. F. *et al. Climate change 2013 the physical science basis: Working Group I contribution to the fifth assessment report of the intergovernmental panel on climate change*. *Climate Change 2013 the Physical Science Basis: Working Group I Contribution to the Fifth Assessment Report of the Intergovernmental Panel on Climate Change* vol. 9781107057 (2013).

147. Větrovský, T. & Baldrian, P. The variability of the 16S rRNA gene in bacterial genomes and its consequences for bacterial community analyses. *PLoS One* **8**, e57923 (2013).

148. Davis, K. E. R., Sangwan, P. & Janssen, P. H. Acidobacteria, Rubrobacteridae and Chloroflexi are abundant among very slow-growing and mini-colony-forming soil bacteria. *Environ. Microbiol.* **13**, 798–805 (2011).

Footnotes

Etymological information:

Candidatus Edaphomicrobium (E.da.pho.mi.cro'bi.um. Gr. neut. n. *edaphos*, soil; N.L. neut. n. *microbium*, a microbe; N. L. neut. n. *Edaphomicrobium*, a soil microbium)

Candidatus Edaphomicrobium janssenii (jans.sen'i.i. N.L. gen. n. *janssenii*, of Janssen, named after Peter H. Janssen, for his pioneering isolation-based studies that first described this lineage [148])

Candidatus Edaphomicrobiaceae (former candidate Chloroflexota family CSP1-4) (E.da.pho.mi.cro.bi.a.ce'ae. N.L. neut. n. *Edaphomicrobium* a (Candidatus) bacterial genus; suff. -*aceae* ending to denote a family; N.L. fem. pl. n. *Edaphomicrobiaceae*, family of the genus *Edaphomicrobium*)

Candidatus Edaphomicrobiales (former candidate Chloroflexota order CSP1-4) (E.da.pho.mi.cro.bi.a'les. N.L. neut. n. *Edaphomicrobium* a (Candidatus) bacterial genus; suff. -*ales* ending to denote an order; N.L. fem. pl. n. *Edaphomicrobiales*, order of the family *Edaphomicrobiaceae*)

Candidatus Edaphomicrobia (former candidate Chloroflexota class Ellin6529) (E.da.pho.mi.cro'bi.a. N.L. neut. n. *Edaphomicrobium* a (Candidatus) bacterial genus; -*ia* ending to denote a class; N.L. neut. pl. n. *Edaphomicrobia*, class of the order *Edaphomicrobiales*)

Candidatus Aridivita (A.ri.di.vi'ta. L. masc. adj. *aridus*, dry; L. fem. n. *vita*, life; N.L. fem. n. *Aridivita*, a dry life)

Candidatus Aridivita willemsiae (wil.lems'i.ae. N.L. gen. n. *willemsiae*, of Willems, named after Anne Willems, for her contributions to Antarctic microbiology using isolation-based approaches)

Candidatus Aridivitaceae (A.ri.di.vi.ta.ce'ae. N.L. neut. n. *Aridivita* a (Candidatus) bacterial genus; suff. -aceae ending to denote a family; N.L. fem. pl. n. *Aridivitaceae*, family of the genus *Aridivita*)

Candidatus Aridivitales (A.ri.di.vi.ta'les. N.L. neut. n. *Aridivita* a (Candidatus) bacterial genus; -ales ending to denote an order; N.L. fem. pl. n. *Aridivitales*, order of the family *Aridivitaceae*)

Candidatus Aridivitia (former candidate Actinobacteriota class UBA4738) (A.ri.di.vi'ti.a. N.L. neut. n. *Aridivita* a (Candidatus) bacterial genus; -ia ending to denote a class; N.L. neut. pl. n. *Aridivitia*, class of the order *Aridivitales*)

Data availability statement:

All amplicon sequencing data, raw metagenomes, and metagenome-assembled genomes were deposited to the NCBI Sequence Read Archive under BioProject accession PRJNA630822.

Acknowledgements:

This study was supported by an ARC DECRA Fellowship (DE170100310; awarded to C.G.), an Australian Antarctic Division grant (4592; awarded to C.G. and S.L.C.), a South African National Antarctic Program grant (110730: awarded to D.A.C), an NHMRC EL2 Fellowship (APP1178715; salary for C.G.), an Australian Government Research Training Stipend Scholarship and a Monash International Tuition Scholarship (awarded to P.M.L. and S.K.B.), and a National Research Foundation SANAP postdoctoral grant (awarded to M.O.). Logistic and financial support for the field work was provided by Antarctica New Zealand and the New Zealand Antarctic Research Institute, respectively (awarded to I.D.H.). We acknowledge the PhD student research discount offered by the Environmental Analysis Laboratory (EAL), a Southern Cross University NATA (National Association of Testing Authorities) ISO17025 accredited commercial and research support facility. We thank Thanavit Jirapanjawat for technical support, Maria Chuvochina for etymological advice, and Andrew Lovering, Philipp Nauer, Eleonora Chiri, Ricardo Cavicchioli, and Belinda Ferrari for helpful discussions.

Author contributions:

D.A.C., C.G., M.O., S.L.C., and I.D.H. conceived this study. C.G. and D.A.C. supervised this study. C.G., P.M.L., D.A.C., and M.O. designed experiments. P.M.L. and G.S. performed experiments. P.M.L., C.G., R.G., G.S., M.O., and D.A.C. analyzed data. P.M.L., C.G., R.G., D.A.C., M.O., and S.L.C. wrote the manuscript with input from all authors. Different authors were specifically responsible for the original sampling campaign (D.A.C., I.D.H.), metagenomic sequencing and assembly (P.M.L., C.G.), community analysis (P.M.L., G.S., C.G.), metabolic annotation

1052 (P.M.L., C.G., M.O., D.A.C.), phylogenetic analysis (C.G., P.M.L., M.O., D.A.C.,
1053 S.K.B.), genetic organization analysis (P.M.L., R.G., C.G., M.O., D.A.C.), molecular
1054 modelling (R.G., C.G.), biogeochemical analysis (P.M.L., C.G., G.S.), and
1055 physicochemical analysis (P.M.L., C.G.). K.J., S.V., M.V.G. and T.M. provided
1056 theoretical and logistical support.
1057
1058 The authors declare no conflict of interest.

Figures

Figure 1. Abundance, composition, and diversity of the microbial communities from the Mackay Glacier region. (a) Boxplot showing the estimated abundance of bacterial and archaeal taxa, based on 16S rRNA copy number determined by quantitative PCR. **(b)** Stacked bar chart showing phylum-level community composition based on metagenomic reads of the single-copy marker gene *rplP* and metagenome-assembled genomes. Bacterial and archaeal taxonomy is based on Genome taxonomy database (GTDB) release 05-RS95. Phyla with less than 1% abundance in the sample were grouped to "Other phyla". **(c)** Boxplot showing alpha diversity (Observed richness, Chao1, Shannon, Faith's phylogenetic diversity) of microbial communities based on 16S rRNA gene amplicon sequence variants. **(d)** Beta diversity of rarefied 16S rRNA gene amplicon sequencing data based on Bray-Curtis dissimilarity and visualised by a non-metric multidimensional scaling ordination (NMDS) plot.

Figure 2. Metabolic potential of the microbial communities to use inorganic compounds, organic compounds, and light for energy and carbon acquisition. Homology-based searches were used to identify signature genes encoding enzymes associated with (from top to bottom): oxidative phosphorylation, trace gas oxidation, sulfur compound oxidation, nitrification, other oxidative processes, photosynthesis, and carbon fixation. The left heatmap shows the percentage of total community members predicted to encode each signature metabolic gene. To infer abundance, read counts were normalized to gene length and the abundance of single-copy marker genes. The right heatmap shows the presence of these genes across the 451 metagenome-assembled genomes spanning 18 phyla. Abundance was normalized by predicted MAG completeness.

Figure 3. Identification of the novel group 1l family of [NiFe] hydrogenases widespread in the Antarctic soil bacterial communities. (a) Maximum-likelihood phylogenetic tree showing the sequence divergence of group 1 [NiFe] hydrogenases identified in MAGs from this study. Amino acid sequences retrieved from the reconstructed genomes were aligned against reference sequences (bootstrapped

with 50 replicates). Branches of group 1 [NiFe] hydrogenases are shaded according to the subgroup classification and tips are colored based on phylum-level affiliation of the sequence. All sequences from MAGs of the Mackay Glacier region clustered with either the well-characterized group 1h [NiFe]-hydrogenases or the previously unreported group 1l [NiFe]-hydrogenases. **(b)** Representative genetic organization of group 1l [NiFe] hydrogenase gene cluster derived from the Antarctic bacterium *Hymenobacter roseosalivarius*. This shows the predicted open reading frames for the large (HylL) and small (HylS) hydrogenase subunits, the five interposing short predicted transmembrane proteins (HylTM1-5), a predicted electron-relaying Rieske-type protein (HylE), and a maturation endopeptidase (HupD). Conserved open reading frames with no predicted function are shown but not labelled. **(c)** Three-dimensional model of the group 1l [NiFe] hydrogenase. This shows a structural homology model of a heterotetramer of HylL and HylS subunits as a ribbon representation and a cartoon of a speculative complex between the hydrogenase and genetically associated HylTM proteins. **(d)** The location of conserved residues coordinating the [NiFe]-centre of the HylL subunit and [FeS] clusters of the HylS subunit of the group 1l [NiFe] hydrogenase. **(e)** Putative location of [FeS] clusters and [NiFe] centre (spheres) in one half of the group 1l [NiFe] hydrogenase tetramer, with conserved coordinating residues (sticks) color coded as in panel C.

Figure 4. Rates of atmospheric trace gas oxidation by soils sampled from the Mackay Glacier region. Boxplots show rates of oxidation of atmospheric H_2, CO, and CH_4 for each soil in duplicate soil microcosms at 10°C, based on gas chromatography measurements. Only rates for samples with detectable gas oxidation are shown. **(a)** Atmospheric gas oxidation rate for each microcosm normalized to wet weight of soil. **(b)** Cell-specific reaction rates for each microcosm. These rates were calculated by dividing the estimated soil cell abundance and proportion of gas oxidizers based on quantitative qPCR and metagenome short read analysis (HhyL and HylL abundance for H_2, CoxL abundance for CO, PmoA and MmoX abundance for CH_4).

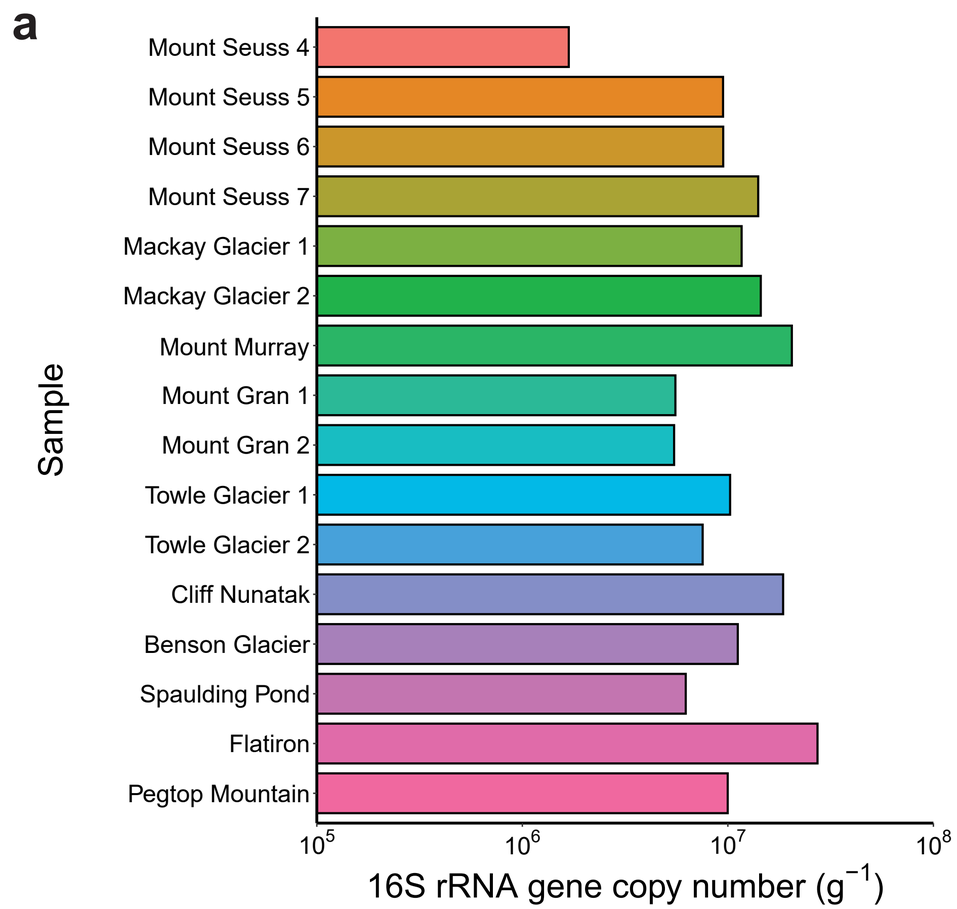

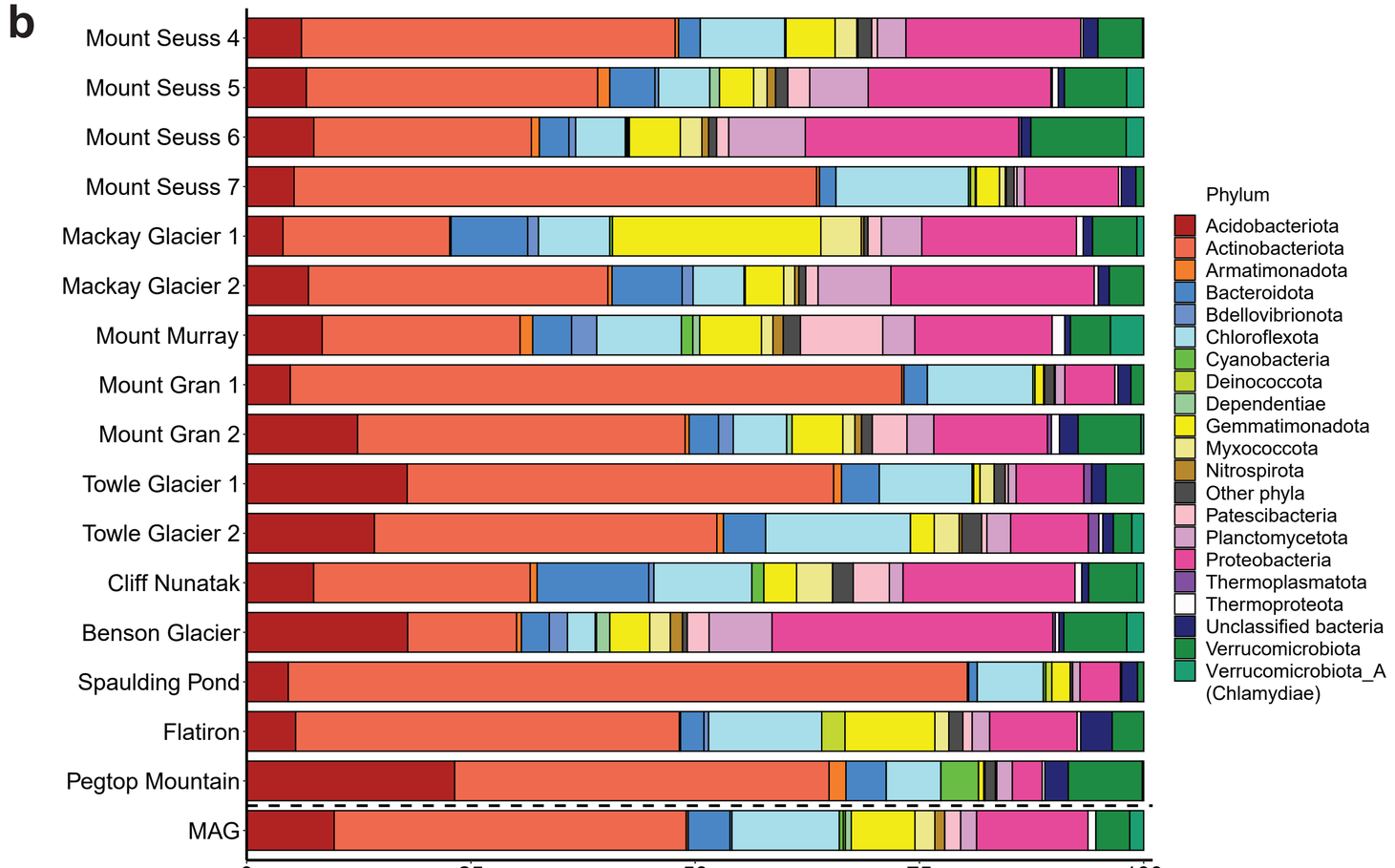

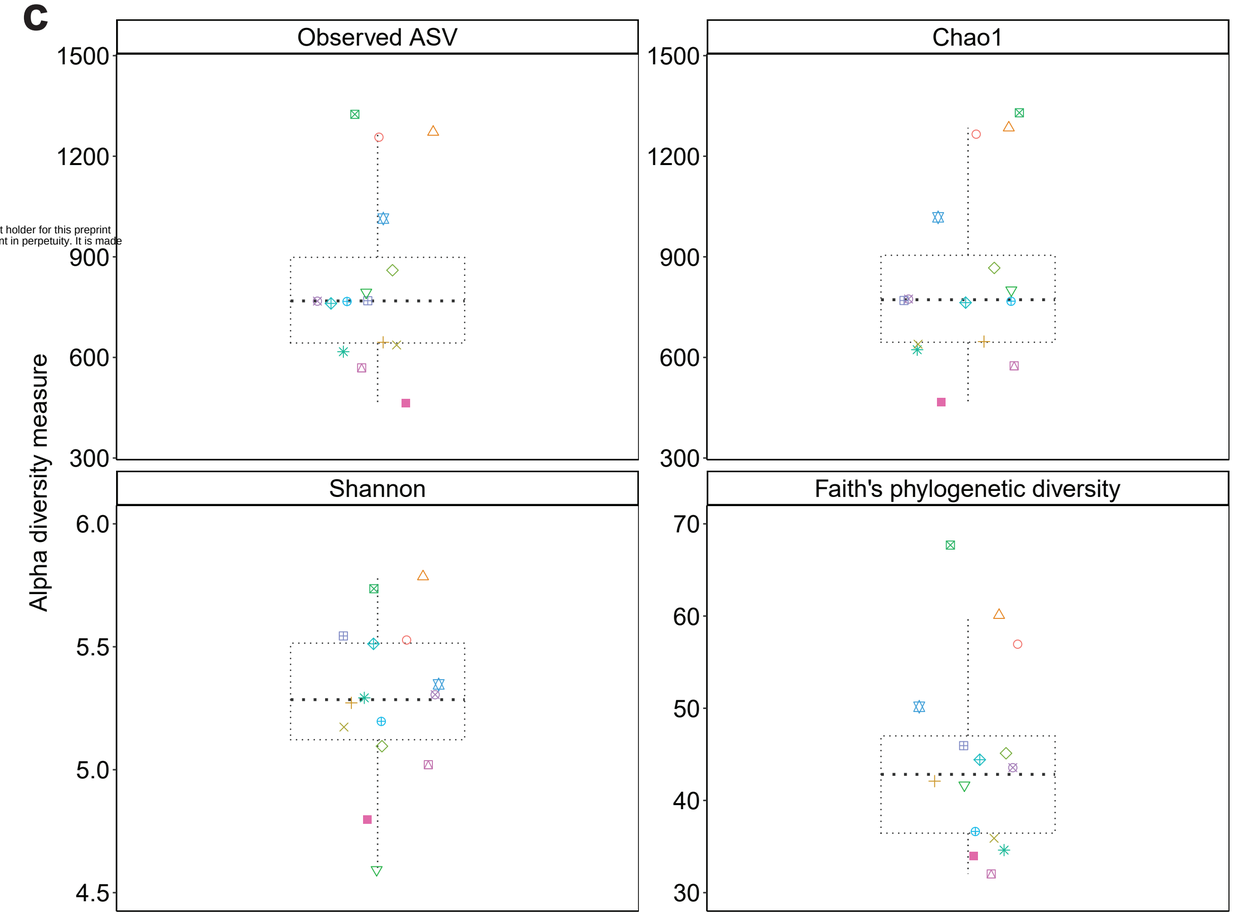

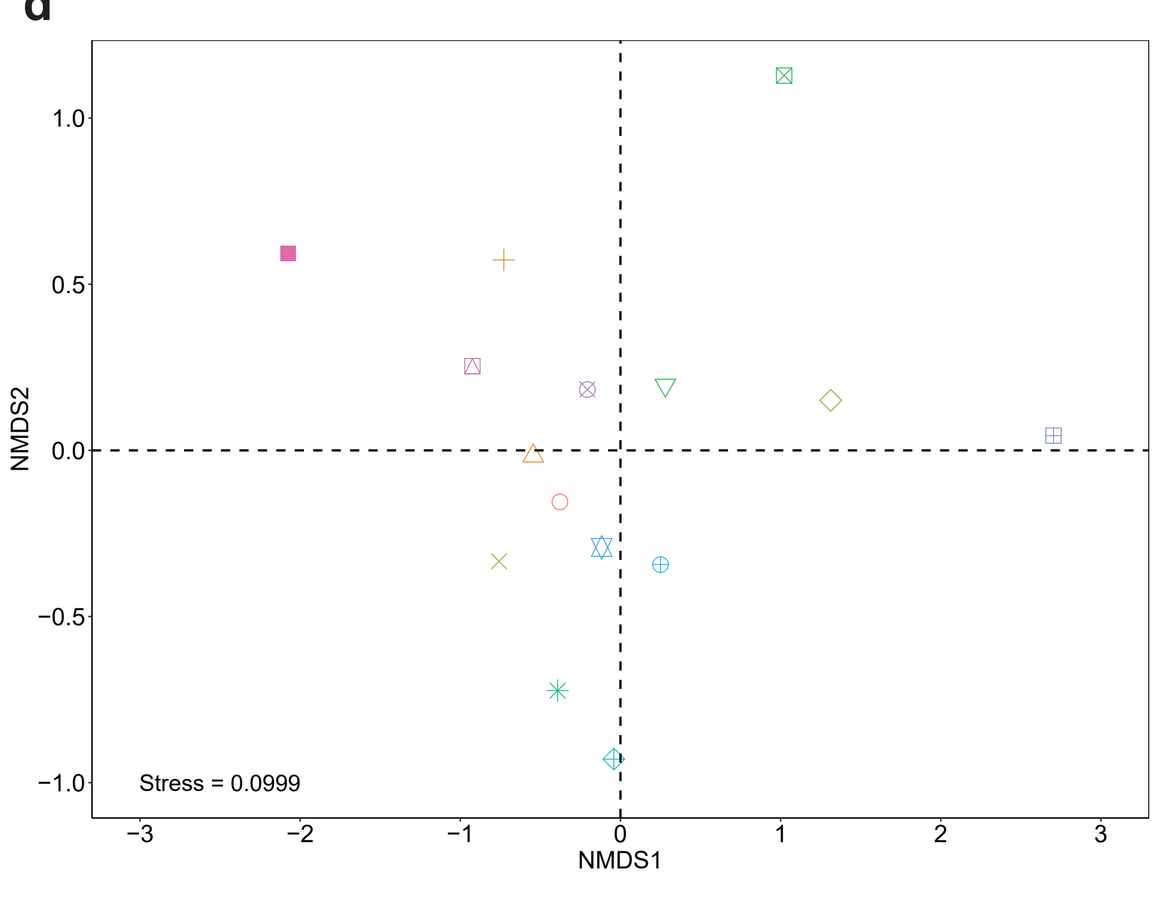

Metabolism	Gene
Oxidative phosphorylation	AtpA
Aerobic respiration	CcoN
Aerobic respiration	CoxA
Aerobic respiration	CydA
Aerobic respiration	CyoA
NADH oxidation	NuoF
Succinate oxidation	SdhA
Anaerobic carbon monoxide oxidation	CooS
Aerobic carbon monoxide oxidation	CoxL
Hydrogen oxidation	[NiFe]-1h
Hydrogen oxidation	[NiFe]-1l
Methane oxidation	MmoA
Methane oxidation	PmoA
Isoprene oxidation	IsoA
Sulfide oxidation	FCC
Sulfide oxidation	Sqr
Thiosulfate oxidation	SoxB
Ammonia oxidation	AmoA
Nitrite oxidation	NxrA
Arsenite oxidation	ARO
Iron oxidation	Cyc2
Formate oxidation	FdhA
Photosystem I−dependent phototrophy	PsaA
Photosystem II−dependent phototrophy	PsbA
Rhodopsin−dependent phototrophy	RHO
Reductive tricarboxylic acid cycle	AclB
Wood−Ljungdahl pathway	AcsB
Crenarchaeotal 4−hydroxylbutyrate cycle	HbsC
Thaumarchaeotal 4−hydroxylbutyrate cycle	HbsT
3−hydroxylpropionate cycle	Mcr
Calvin−Benson−Bassham cycle	RbcL

Metagenome

Mount Seuss 4
Mount Seuss 5
Mount Seuss 6
Mount Seuss 7
Mackay Glacier 1
Mackay Glacier 2
Mount Murray
Mount Gran 1
Mount Gran 2
Towle Glacier 1
Towle Glacier 2
Cliff Nunatak
Benson Glacier
Spaulding Pond
Flatiron
Pegtop Mountain

MAG (Phylum−level)

Acidobacteriota (44)
Actinobacteriota (177)
Armatimonadota (1)
Bacteroidota (21)
Bdellovibrionota (1)
Chloroflexota (54)
Cyanobacteria (2)
Deinococcota (1)
Dependentiae (3)
Gemmatimonadota (32)
Myxococcota (10)
Nitrospirota (5)
Patescibacteria (8)
Planctomycetota (8)
Proteobacteria (56)
Verrucomicrobiota (17)
Verrucomicrobiota_A (7)
Thermoproteota (4)

0 25 50 75 100
Estimated abundance in community (%)

a

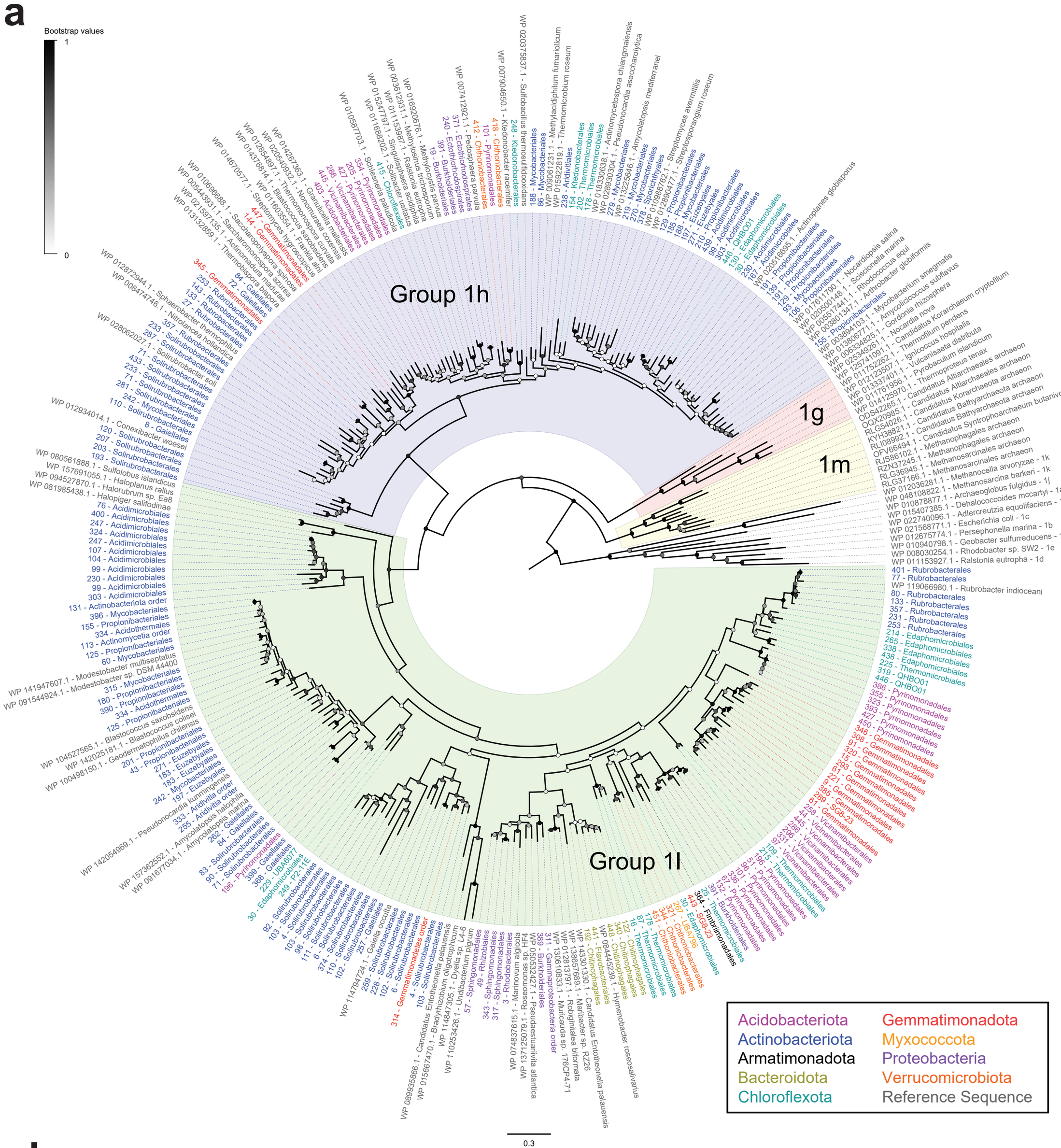
Bootstrap values
1
0
Group 1h
1g
1m
Group 1l
WP 020375837.1 - Sulfobacillus thermosulfidooxidans
248 - Ktedonobacterales
188 - Mycobacteriales
86 - Mycobacteriales
WP 009061231.1 - Methylacidiphilum fumariolicum
WP 015922819.1 - Thermomicrobium roseum
238 - Aridivitiales
154 - Ktedonobacterales
202 - Thermomicrobiales
178 - Thermomicrobiales
WP 018330638.1 - Actinomycetospora chiangmaiensis
WP 028930304.1 - Pseudonocardia asaccharolytica
279 - Mycobacteriales
WP 013225646.1 - Amycolatopsis mediterranei
219 - Mycobacteriales
270 - Mycobacteriales
378 - Sporichthyales
WP 012890477.1 - Streptomyces avermitilis
WP 010988762.1 - Streptosporangium roseum
129 - Propionibacteriales
185 - Propionibacteriales
188 - Mycobacteriales
197 - Euzebyales
271 - Euzebyales
210 - Propionibacteriales
439 - Acidimicrobiales
99 - Acidimicrobiales
303 - Acidimicrobiales
446 - QHBO01
130 - Edaphomicrobiales
30 - Edaphomicrobiales
230 - Acidimicrobiales
167 - Acidimicrobiales
WP 020516695.1 - Actinoplanes globisporus
191 - Propionibacteriales
139 - Propionibacteriales
191 - Propionibacteriales
129 - Mycobacteriales
93 - Propionibacteriales
106 - Propionibacteriales
WP 017611790.1 - Nocardiopsis salina
WP 020500148.1 - Sciscionella marina
WP 005517441.1 - Rhodococcus equi
WP 003801347.1 - Arthrobacter globiformis
155 - Propionibacteriales
WP 003894103.1 - Mycobacterium smegmatis
WP 013806771.1 - Amycolicicoccus subflavus
WP 006334825.1 - Gordonia rhizosphera
WP 025349261.1 - Nocardia nova
WP 125741091.1 - Candidatus Korarchaeum cryptofilum
WP 011752262.1 - Thermofilum pendens
WP 012123507.1 - Ignicoccus hospitalis
WP 013337401.1 - Pyrobaculum islandicum
WP 011761966.1 - Vulcanisaeta distributa
WP 014125970.1 - Thermoproteus tenax
ODS42265.1 - Candidatus Altiarchaeales archaeon
OQX20985.1 - Candidatus Altiarchaeales archaeon
RLG54026.1 - Candidatus Korarchaeota archaeon
KYH38821.1 - Candidatus Bathyarchaeota archaeon
RLI08992.1 - Candidatus Syntrophoarchaeum butanivorans
OFV66494.1 - Methanophagales archaeon
RJS86102.1 - Methanophagales archaeon
RZN37245.1 - Methanosarcinales archaeon
RLG36945.1 - Methanosarcinales archaeon
RLG37166.1 - Methanocella arvoryzae - 1k
WP 012036281.1 - Methanosarcina barkeri - 1k
WP 048108822.1 - Methanoregula formicica - 1j
WP 010878877.1 - Archaeoglobus fulgidus - 1i
WP 015407385.1 - Dehalococcoides mccartyi - 1a
WP 022740096.1 - Adlercreutzia equolifaciens - 1c
WP 021568771.1 - Escherichia coli - 1b
WP 012675774.1 - Persephonella marina - 1d
WP 010940798.1 - Geobacter sulfurreducens - 1f
WP 008030254.1 - Rhodobacter sp. SW2 - 1e
WP 011153927.1 - Ralstonia eutropha - 1d
401 - Rubrobacterales
77 - Rubrobacterales
WP 119066980.1 - Rubrobacter indioceani
80 - Rubrobacterales
133 - Rubrobacterales
357 - Rubrobacterales
231 - Rubrobacterales
253 - Rubrobacterales
214 - Edaphomicrobiales
265 - Edaphomicrobiales
338 - Edaphomicrobiales
438 - Edaphomicrobiales
225 - Thermomicrobiales
319 - QHBO01
446 - QHBO01
386 - Pyrinomonadales
355 - Pyrinomonadales
323 - Pyrinomonadales
393 - Pyrinomonadales
427 - Pyrinomonadales
450 - Pyrinomonadales
346 - Pyrinomonadales
308 - Gemmatimonadales
91 - Gemmatimonadales
320 - Gemmatimonadales
15 - Gemmatimonadales
293 - Gemmatimonadales
61 - Gemmatimonadales
221 - Gemmatimonadales
385 - Gemmatimonadales
299 - SG8-23
61 - Gemmatimonadales
258 - Gemmatimonadales
445 - Vicinamibacterales
286 - Vicinamibacterales
331 - Vicinamibacterales
97 - Vicinamibacterales
109 - Thermomicrobiales
215 - Pyrinomonadales
196 - Pyrinomonadales
51 - Pyrinomonadales
96 - Pyrinomonadales
101 - Pyrinomonadales
336 - Pyrinomonadales
67 - Pyrinomonadales
132 - Pyrinomonadales
391 - Burkholderiales
25 - Thermomicrobiales
364 - Fimbriimonadales
443 - SG8-23
30 - Edaphomicrobiales
267 - UBA796
321 - Chthoniobacterales
344 - Chthoniobacterales
451 - Chthoniobacterales
178 - Thermomicrobiales
87 - Thermomicrobiales
16 - Thermomicrobiales
122 - Chitinophagales
340 - Chitinophagales
448 - Chitinophagales
WP 084445239.1 - Hymenobacter roseosalivarius
441 - Flavobacteriales
192 - Chitinophagales
WP 143301330.1 - Candidatus Entotheonella palauensis
WP 138657689.1 - Maribacter sp. RZ26
WP 012813797.1 - Robiginitalea biformata
WP 130610833.1 - Muricauda sp. 176CP4-71
311 - Gammaproteobacteria order
389 - Burkholderiales
WP 050532427.1 - Pseudaestuariivita atlantica
WP 137125079.1 - Roseomonas sp. HF4
WP 074837615.1 - Marinovum algicola
3 - Rhodobacterales
343 - Sphingomonadales
317 - Sphingomonadales
49 - Rhizobiales
57 - Sphingomonadales
WP 110253426.1 - Dyella sp. L4-6
WP 114847305.1 - Bradyrhizobium oligotrophicum
WP 015667470.1 - Candidatus Entotheonella palauensis
WP 089935866.1 - Candidatus Entotheonella palauensis
103 - Solirubrobacterales
4 - Solirubrobacterales
102 - Solirubrobacterales
6 - Solirubrobacterales
228 - Solirubrobacterales
259 - Solirubrobacterales
257 - Gaiellales
WP 114794724.1 - Gaiella occulta
314 - Gemmatimonadetes order
110 - Solirubrobacterales
374 - Solirubrobacterales
111 - Solirubrobacterales
6 - Solirubrobacterales
98 - Solirubrobacterales
103 - Solirubrobacterales
4 - Solirubrobacterales
103 - Solirubrobacterales
92 - Solirubrobacterales
249 - P2-11E
229 - UBA6077
368 - Gaiellales
399 - Gaiellales
196 - Pyrinomonadales
71 - Solirubrobacterales
90 - Solirubrobacterales
83 - Solirubrobacterales
84 - Gaiellales
262 - Gaiellales
255 - Aridivitia order
333 - Aridivitia order
WP 091677034.1 - Amycolatopsis marina
WP 157362552.1 - Amycolatopsis halophila
WP 142054969.1 - Pseudonocardia kunmingensis
197 - Euzebyales
242 - Mycobacteriales
183 - Euzebyales
271 - Euzebyales
43 - Propionibacteriales
201 - Propionibacteriales
WP 100498150.1 - Geodermatophilus chilensis
WP 142025181.1 - Blastococcus colisei
WP 104527565.1 - Blastococcus saxobsidens
125 - Propionibacteriales
334 - Acidothermales
390 - Propionibacteriales
180 - Propionibacteriales
315 - Mycobacteriales
WP 091544924.1 - Modestobacter sp. DSM 44400
WP 141947607.1 - Modestobacter multiseptatus
60 - Mycobacteriales
125 - Propionibacteriales
113 - Actinomycetia order
334 - Acidothermales
155 - Propionibacteriales
396 - Mycobacteriales
131 - Actinobacteriota order
99 - Acidimicrobiales
303 - Acidimicrobiales
99 - Acidimicrobiales
230 - Acidimicrobiales
99 - Acidimicrobiales
400 - Acidimicrobiales
247 - Acidimicrobiales
324 - Acidimicrobiales
247 - Acidimicrobiales
107 - Acidimicrobiales
104 - Acidimicrobiales
76 - Acidimicrobiales
WP 081985438.1 - Halopiger salifodinae
WP 094527870.1 - Halorubrum sp. Ea8
WP 157691055.1 - Haloplanus rallus
WP 080561888.1 - Sulfolobus islandicus
193 - Solirubrobacterales
203 - Solirubrobacterales
207 - Solirubrobacterales
120 - Solirubrobacterales
WP 012934014.1 - Conexibacter woesei
8 - Gaiellales
242 - Mycobacteriales
281 - Solirubrobacterales
71 - Solirubrobacterales
233 - Solirubrobacterales
433 - Solirubrobacterales
71 - Solirubrobacterales
287 - Solirubrobacterales
WP 028062027.1 - Solirubrobacter soli
357 - Rubrobacterales
133 - Rubrobacterales
27 - Rubrobacterales
143 - Rubrobacterales
253 - Rubrobacterales
84 - Gaiellales
72 - Gaiellales
345 - Gemmatimonadales
WP 008474746.1 - Nitrolancea hollandica
WP 012872944.1 - Sphaerobacter thermophilus
WP 013132859.1 - Thermobispora bispora
WP 021597135.1 - Saccharomonospora azurea
WP 005443931.1 - Saccharopolyspora spinosa
WP 014670577.1 - Actinomadura madurae
447 - Gemmatimonadales
144 - Gemmatimonadales
WP 012854897.1 - Streptomyces hygroscopicus
WP 011603554.1 - Thermomonospora curvata
WP 020540932.1 - Blastococcus saxobsidens
WP 014376814.1 - Nonomuraea coxensis
WP 014267363.1 - Granulicella mallensis
403 - Acidobacteriales
445 - Vicinamibacterales
286 - Vicinamibacterales
427 - Pyrinomonadales
205 - Pyrinomonadales
354 - Pyrinomonadales
WP 010587703.1 - Schlesneria paludicola
WP 010696688.1 - Frankia alni
WP 011682202.1 - Solibacter usitatus
415 - Chloroflexales
WP 015247797.1 - Singulisphaera acidiphila
WP 003612931.1 - Ralstonia eutropha
WP 011153987.1 - Methylosinus trichosporium
WP 016920676.1 - Methylocystis parvus
19 - Burkholderiales
391 - Burkholderiales
240 - Ectothiorhodospirales
371 - Ectothiorhodospirales
WP 007412921.1 - Pedosphaera parvula
412 - Chthoniobacterales
101 - Pyrinomonadales
418 - Chthoniobacterales
WP 007904650.1 - Ktedonobacter racemifer
Acidobacteriota
Actinobacteriota
Armatimonadota
Bacteroidota
Chloroflexota
Gemmatimonadota
Myxococcota
Proteobacteria
Verrucomicrobiota
Reference Sequence
0.3

b

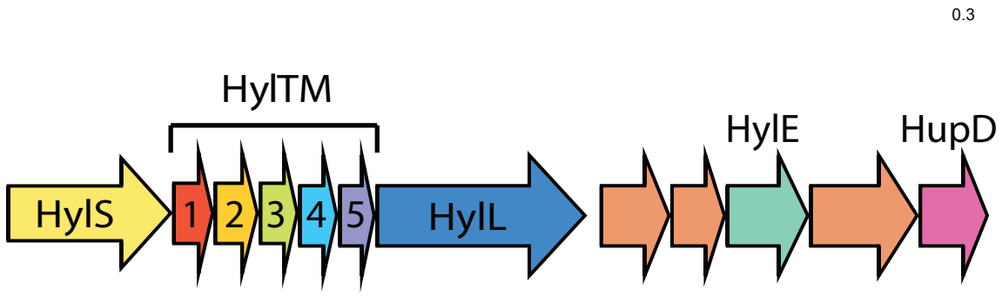
HylTM
HylS
1
2
3
4
5
HylL
HylE
HupD

c

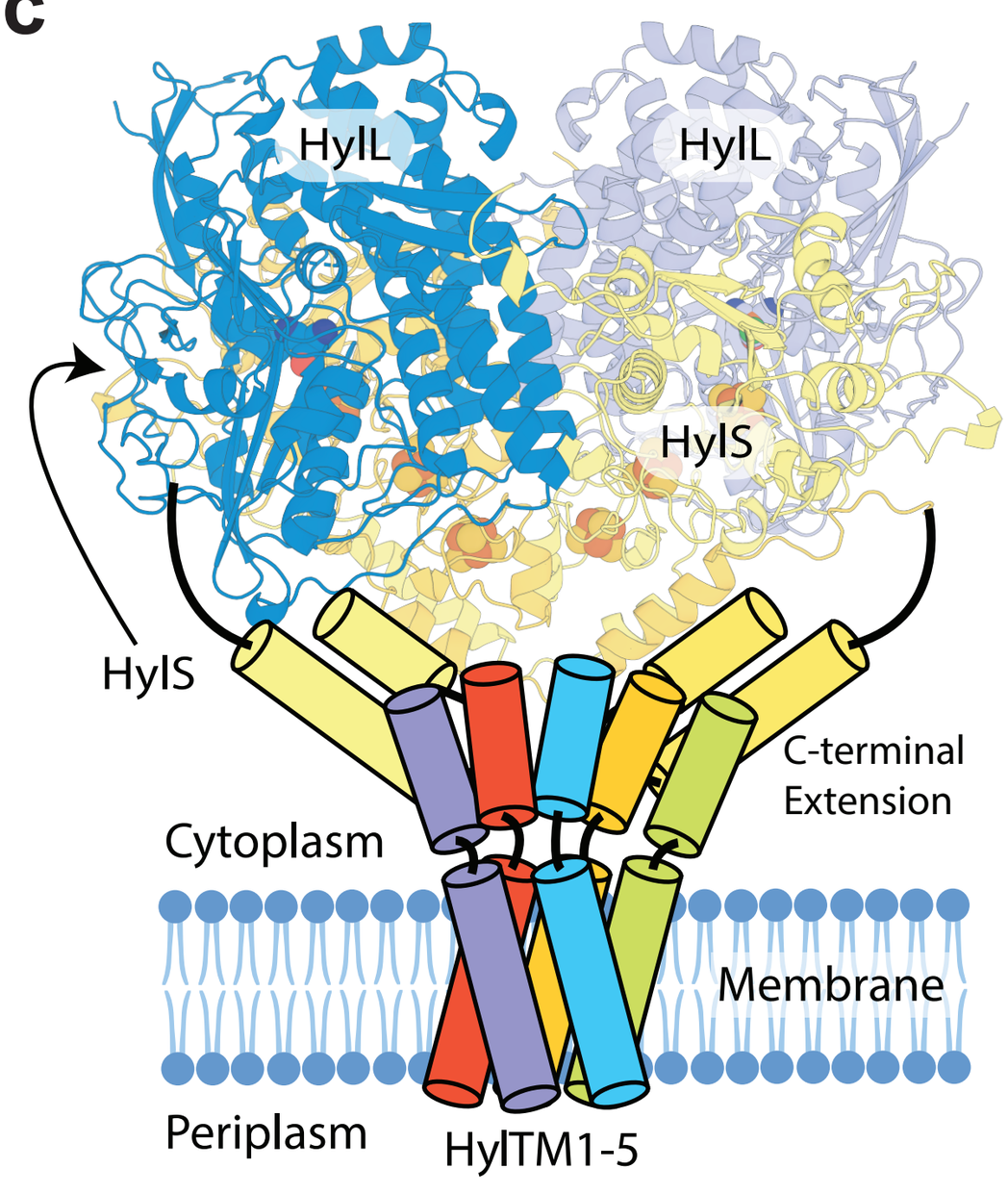
HylL
HylL
HylS
HylS
C-terminal
Extension
Cytoplasm
Membrane
Periplasm
HylTM1-5

d

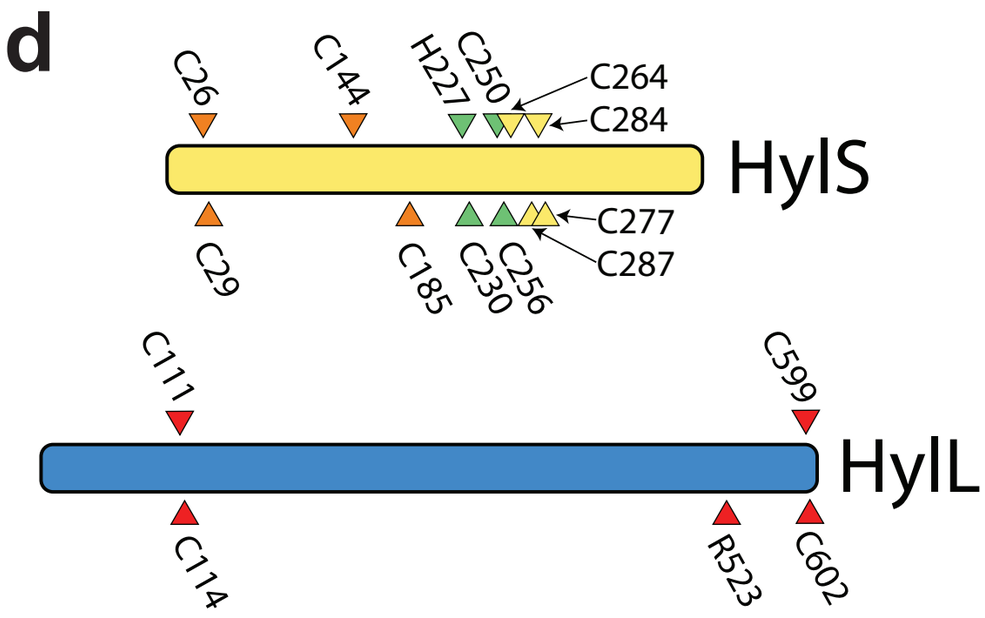
C26
C144
H227
C250
C264
C284
HylS
C29
C185
C230
C256
C277
C287
C111
C599
HylL
C114
R523
C602

e

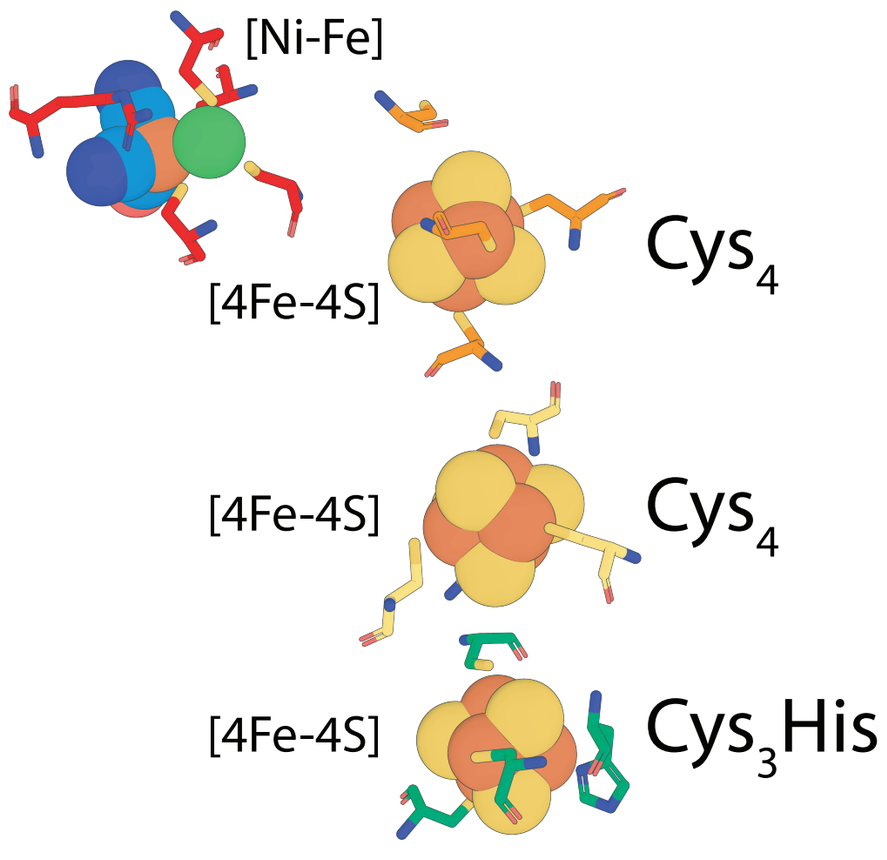
[Ni-Fe]
[4Fe-4S]
Cys4
[4Fe-4S]
Cys4
[4Fe-4S]
Cys3His

a

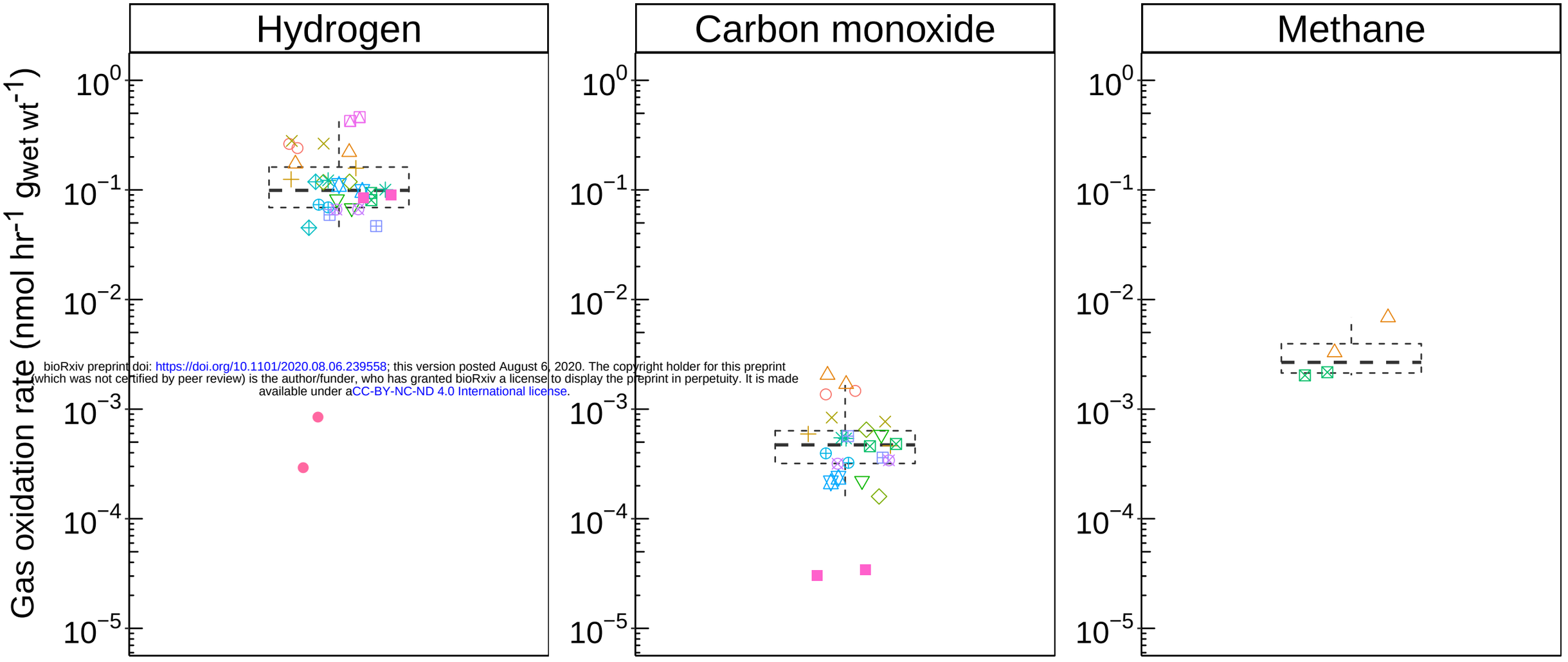

b